2022-09

Photocatalytic degradation of azo dyes in textile wastewater by Polyaniline composite catalyst-a review

Oyetade, Joshua

Elsevier B.V.

https://doi.org/10.1016/j.sciaf.2022.e01305

Scientific African 17 (2022) e01305

Contents lists available at ScienceDirect

Scientific African

journal homepage: www.elsevier.com/locate/sciaf

Photocatalytic degradation of azo dyes in textile wastewater by Polyaniline composite catalyst-a review

Joshua Akinropo Oyetade*, Revocatus Lazaro Machunda, Askwar Hilonga

School of Materials, Energy, Water and Environmental Science, Nelson Mandela African Institution of Science and Technology, PO Box 447, Arusha, Tanzania

ARTICLE INFO

Article history:
Received 13 February 2022
Revised 1 June 2022
Accepted 28 July 2022

Editor: DR B Gyampoh

Keywords:
Azo
Polyaniline
Photocatalysis
Photon
Wastewater
Nanocomposite

ABSTRACT

Azo dyes in industrial textile and dye effluent (5–30%) have become irresistibly recalcitrant and toxic to both treatments and the environment respectively. Global concerns about the persistent nature of these dyes and the limitation of the conventional treatment currently in place have led to this critical analysis and evaluation of the photocatalytic approach using nano-technology. The review of literature has indicated that although this approach is effective, however, the limitation of frequent electron-hole recombination during the process coupled with challenges of agglomeration of nano particle powder, photo-corrosion and photosensitivity of the various nano-materials are still challenges associated with the development of polymeric based nano composite catalyst of polyaniline (PANI). The unique features of incredible charge transport properties, surface morphology and enhanced functional properties gave PANI the choice of use among other conductive polymers for composite fabrication with materials such TiO_2, *and* ZnO_2, *Graphene oxides*, *CNTs*. Photoactive properties, conductivity mechanical, thermal and chemical stability equally offers the polymer the propensity of bandgap tunability when in composites with other materials. Consequently, effective recovery and reuse of the composite catalyst for more than four runs with efficiency > 90% becomes obtainable. These appreciable advantages offer fabricated nano composite polymeric-based catalysts an effective outlook of use in the remediation of toxic azo dyes industrially as compared to the bio-catalyst and pure nano adsorbent materials. Therefore, the review discusses the treatment process for azo dyes, fabrication and performance evaluation of improved composite catalyst of PANI as an alternative to the conventional catalyst in wastewater and recommends for further investigation in PANI to enhance treatability of azo dyes.

Introduction

Azo dyes are identified with one or more azo bond linkage (-N=N-) having the most prominent use of 70% among over 2,000 species of synthetic dyes [1–4,70]. Several studies have been carried out on the properties of these dyes which reveal their unique simplicity in synthesis, excellent fastness rating, high solubility, and uptake by the substrate. These properties

* Corresponding author.
E-mail addresses: oyetadej@nm-aist.ac.tz, joshuaoyetade@gmail.com (J.A. Oyetade).

https://doi.org/10.1016/j.sciaf.2022.e01305

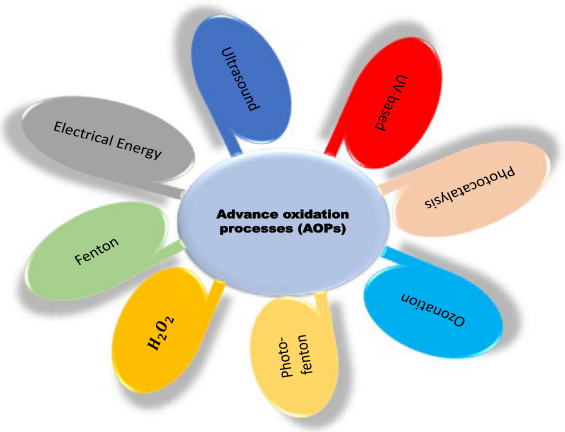

Fig. 1. Advanced oxidation processes (AOPs).

give it a preferential choice of use among other dyes in textile industries (Oyetade et al. [173]). However, these dyes are commonly present in discharged textile wastewater which results in environmental pollution, limiting the quality of life ([9,100]). An estimate of 50,000 tonnes of textile wastewater is annually discharged with 10–30% concertation of unfixed dyes from dyeing, printing, pigmentation, and bleeding of the textile substrate [13], (Adetuyi et al. [175]; Oyetade et al. [174]). The toxic impacts of these dyes in wastewater are based on high resistance to microbial degradation, conventional treatments and chemical transformation of the dye molecules in the effluent to more toxic pollutants (benzidine) [13,27,56]. Although various conventional treatment techniques have been reported. However, limitations of toxic sludge formation, cost and low dye removal efficiency of azo dyes necessitated the use of the improved photocatalytic technique in nanotechnology (10^{-9}) for dye remediation [13,100,142,174]. The process of dye degradation/decolorization via the use of photon-active nanomaterials as adsorbents is called photocatalysis [27,56,124]. Studies have shown the effectiveness of these techniques in azo dye degradation among other processes of advanced oxidation processes (AOPS) (Fig. 1) (Rauf and Ashraf [176]; Pandey et al. [156]). The whole process initiates a redox reaction which spontaneously generates radicals (e.g hydroxides, peroxides, and superoxides) while forming electron-hole pairs. The radicals combine with the organic pollutants (e.g. dyes in wastewater) and mineralize them into compounds such as CO_2 *and* H_2O (Shindhal et al. [150] Pandey et al. [156]).

Although there exists a wide spectrum of nano-photocatalyst materials such as bio-based, metal oxide-based, polymer-based, carbon-based and inorganic-based materials [35,101]. However, the challenges corresponding to their uses as photocatalyst includes photo-corrosion, frequent electron-hole recombination, large band gap, low photon detection and capturing propensity and agglomeration of powdered nano particles (NPs) [6,123,127,130]. These challenges gave rise to the investigation of polymer-based nano-composite from conducting polyaniline (PANI). Conducting polymers such as polyaniline (PANI), polythiophene, polypyrrole, etc., have been known for multiple varieties of applications in electronic devices, sensors, anti-corrosive coatings, energy storage devices, catalysis, etc [101].

Interestingly, out of these varieties of conducting polymers, PANI stands out with a unique applicable potential in photocatalysis [42]. The polymer commonly synthesized by oxidative polymerization exhibits incredible charge transport dynamics which supports its high photon capturing activity and lower band gap [19,72]. Furthermore, it exhibits other unique potentials such as high adsorptive capacity, ability to form polymeric support for nano powder materials with enhanced morphology, tuneability of bandgap on fabrication with other nano materials as composites and high solubility based on its amphiphilicity [59,112,141]. The multifunctional potentials of this polymer in composite fabrication necessitated the study of improved functional potentials and performance evaluation of the polymeric nano composite catalyst. This present paper evaluates the photodegradation performance of PANI nano composite applied to textile wastewater laden with azo dyes as compared to the conventional catalyst as reported in literature.

Azo dyes: properties and classification

Azo dyes are the largest class of synthetic dyes which are commonly synthesized by diazotization and coupling reactions via several chemical routes [16]. Although they can equally be synthesized by Gewald reaction (Fig. 2) however, the most adopted synthetic pathway for these industrial dyes is by diazotization and coupling reaction to give more brilliant shades, optimum yield, desired particle size and improved dispersibility [14,31,47,114].

The process involves the diazotization of a primary aromatic amine, before coupling with electron-rich nucleophiles as described in Fig. 2

Azo dyes structurally consist of one or more azo (−N=N−) chromophoric group(s) and mostly water-soluble sulfonic (SO^{3-}) (Fig. 3a) group which justifies their affinity for water and excellent fastness rating (Sudha et al., [177,90]. These structural features also explain their increasing industrial demands and presence in most textile wastewater). Furthermore,

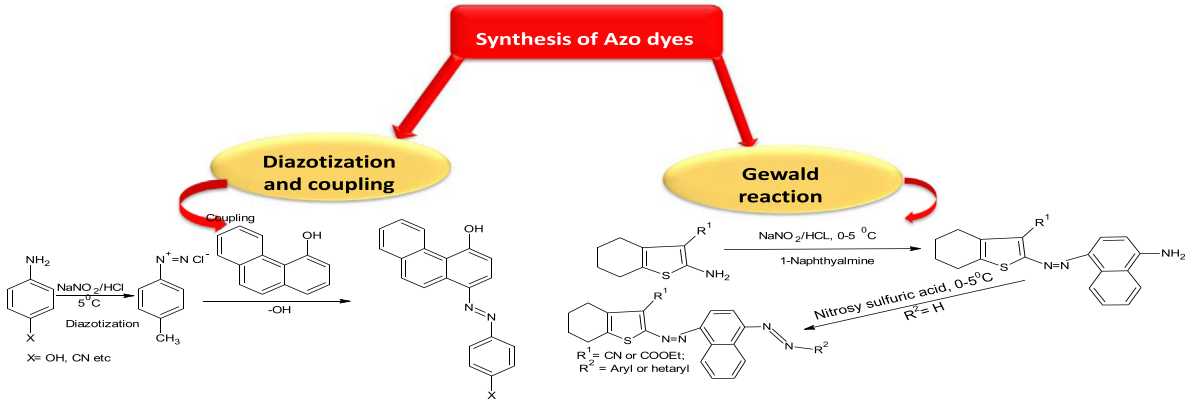

Fig. 2. Synthesis of azo dyes.

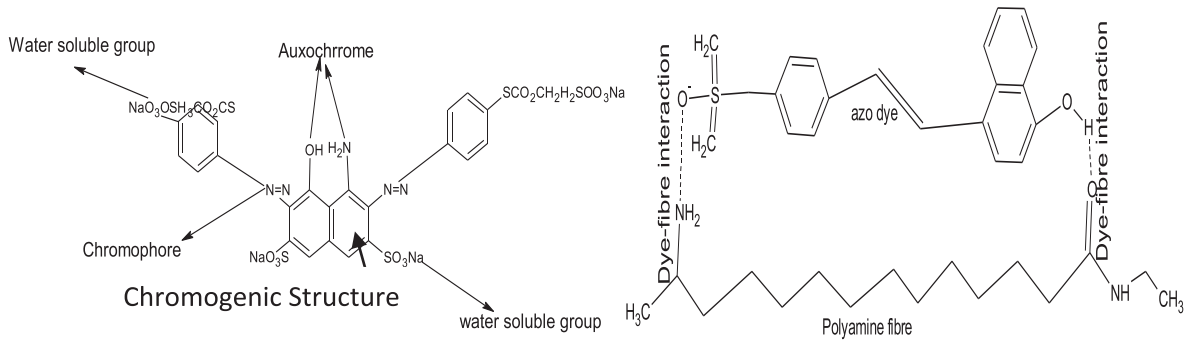

Fig. 3. a: Structure of reactive azo dye. b: Structure of Dye-fibre.

auxochromes linking to phenyl or naphthyl rings such as amine, chloro, hydroxyl, methyl, nitro, sulfonate may be present in their structure which contributes to bathochromic shift thereby enhancing colour intensity (Sudha et al. [177]).

Generally, dyes are classified into two broad categories concerning their application or chemical structure. Classification based on applications separates dyes into groups such as reactive, acid, basic, sulfur dye, mordant, direct, disperse, pigment, vat, and azo dyes (Popoola [90]). While structurally, they can be categorized as, indamine, diphenylmethane, xanthene sulfur, carotenoid, acridine, quinoline, anthraquinone, nitro, azo, indigoid, amino- and hydroxy ketone, phthalocyanine, inorganic pigment, etc. Although based on their charge they may be either anionic, non-ionic, or cationic dyes . However, based on their chemical reactivity they are classed as either acid, basic, reactive, direct or disperse azo dyes [128]. Furthermore, classification concerning azo constituents could be mono azo (one azo group), diazo (two azo groups), triazo (three azo), tretrakisazo (four azo) or more (poly azo) [13]. However, based on their colour index in Table 1, they are classed monozo, diazo, triazo, polyazo and azoic dyes [102]. These varieties of classification, their aromatic constituent(s) and the auxochromic substituent(s) account for their vast application in the textile industries and determine the bonding arrangement with cellulosic, protein, regenerated, and synthetic polymers [90,102]. Popoola [90] and Oyetade et al. [174] added that these dyes have strong dye-fiber interaction (Fig. 3b), which accounts for their excellent fastness rating and resistance to bleeding, crocking and generally running off from the substrate applied.

Industrial applications and environmental impacts of azo dyes

Statistically, they have 70% use among other industrial dyes with applications in paint, paper and most especially textile industries [102]. Despite their vast use, azo dyes remain an industrial dye of global threat. Among the assortment of azo dyes, the most widely used reactive azo dyes are associated with the toxic environmental impact on disposal, and difficulty in the treatment of their corresponding effluents (Jagadeesan et al., 2021). The toxicity of azo dyes stems from the hydrolysis reaction of loose dyes present in textile wastewater after textile substrate application. On discharge, the dye molecules become persistent in the environment and can bio-transform into aromatic amine products with acute mutagenic and carcinogenic effects on the organism (Bruna et al. [178]). Textile effluents laden with azo dyes, especially the commonly used Congo red, methylene blue and green, benzidine may predispose a man to various impaired health effects and hormonal dysfunction such as mutagenesis, quadriplegia, jaundice, cyanosis, tissue necrosis, vomiting chromosomal fractures, carcinogenesis, and respiratory toxicity (Vinothkannan et al. [179]). The toxicological impacts of these dyes are connected to the substituent position and the nature of the dyes (Bruna et al. [178]). Some of these dyes are less toxic but their presence

Table 1
Structural classification of azo dyes and their colour index [13,16,47].

S/N	Types of Azo	Colour Index CI NO	Structural examples
1	Monoazo	11000–99999	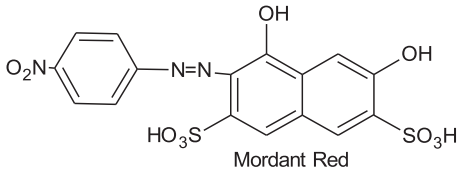 Mordant Red
2	Diazo	20000–29999	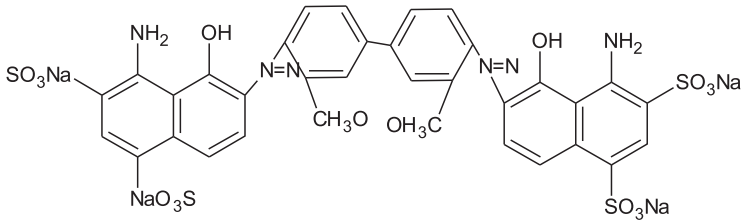
3	Triazo	30000–34999	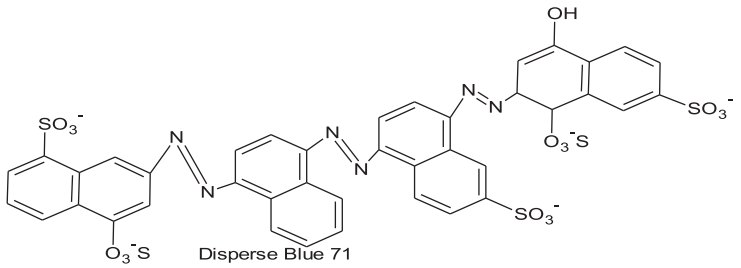 Disperse Blue 71
4	Polyazo	35000–36999	More than two -N=N- groups including triazo
4	Azoic	37000–39999	Same structure only different Colour Index (CI)

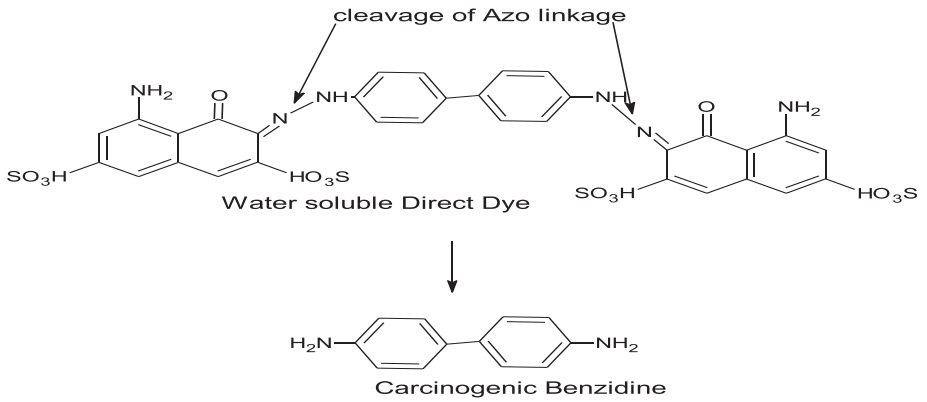

Fig. 4. Bond cleavage of azo dye in textile wastewater.

in wastewater after dyeing, printing, or pigmentation processes may cause a reduction in the azo bond, imparting them with strong mutagenic action (Vinothkannan et al. [179]). For instance, direct black 38 (azodisalecylate) gives a breakdown product like benzidine (Fig. 4) and other derivates such as anilines nitro semis, and dimethyl amines which have carcinogenic inducing effects in humans and animals [100,111]. Furthermore, the presence of these dyes discharged into water bodies constitute a significant reduction of light penetration thereby producing different amine with higher genotoxic and mutagenic effect (Ventura et al. [180]; Bruna et al. [178]).

Treatment process of azo dyes in textile wastewater

Literature has reported and recommended the use of various conventional treatment processes for textile wastewater laden with azo dyes and dyeing auxiliaries. These processes are functionally described as physical, chemical, or biological treatment processes (Table 3) ([148] Ventura et al. [180]; Bruna et al. [178]; Siani, 2017) [111]. Table 2 describes these conventional treatment approaches and their corresponding merits and limitations. Among the treatment technologies, recent

Table 2
Convectional treatment processes textile wastewater.

Treatment approach	Treatment Technologies	Definition	Advantages	Disadvantages	References
Physical	Adsorption	This is a surface reaction in which soluble organic dyes in the wastewater (adsorbate) are transferred unto the porous material (adsorbent). The adhesion of dye molecules unto the surface of the material can be by either physical (physicosorption) or chemical interaction (chemosorption)	Cost-effective Fast Reproducible	Difficulty in adsorbent recovery High cost of removal of toxic sludge	[100]
	Ion exchange	Wastewater is passed through beds of ion exchange resins where the resins selectively allow an exchange for sodium or hydrogen ions of the resin.	Possibility of adsorbent regeneration High selectivity and efficiency	Ineffective method against dispersed dyes Very Expensive	[148]
	Membrane filtration	An advanced technology that uses a pressure-driven membrane to pass wastewater through a porous membrane trapping solute size greater than the pore size of the membrane	Effective for the removal of all dyes High Efficiency	Requires expensive high pressure High Cost of membrane selection Production of excessive sludge	[149,150]
	Coagulation and Flocculation	this involves the aggregation of dye molecules in textile wastewater with flocculants followed by gravitational separation	Easily trap suspended dye particle into flocs The filtrable solution is obtainable Simplest chemical method	It is a process control treatment process High Cost of separation and sludge disposal	[151] Siani et al., 2017

(*continued on next page*)

Table 2 (*continued*)

Treatment approach	Treatment Technologies	Definition	Advantages	Disadvantages	References
Chemical	UV radiation	Treatment of textile wastewater under the influence of radiation sourced from UV lamps working under 253.7 nm.	Simplicity Effective for a wide spectrum of organic dyes	Requires adequate oxygen supply Requires catalysts that can be environmental stressors	Siani et al., 2017
	Electrokinetic coagulation and filtration	It is an advanced electrochemical treatment that involves systematic processes such as electrolytic reactions at electrodes, coagulation of dyes in wastewater and adsorption of soluble pollutants on coagulants before consequent removal by sedimentation	Economic viability Very efficient	Generation of toxic sludge with a high disposal cost High operating cost	[152,153]
	Peroxidation of salts of iron II (Fenton reaction)	A method that uses a mixture of hydrogen peroxide and iron salts (Fe2+) which produces hydroxyl radicals (OH•) in an acidic medium at ambient conditions. The chemistry behind this process is the formation of reactive oxidizing species, able to effectively degrade the pollutants of the effluent and it involves pH adjustment, oxidation, neutralization and coagulation.	Functional for the removal of soluble and insoluble dyes Little energy is required Efficient decolourization of soluble and insoluble dyes Use for High reduction of COD effectively destroys toxic wastes and non-biodegradable compounds	Generation of toxic by-products/sludge	[215]
	Ozonization	The technology uses an oxidizing agent (such as O3, H2O2) in the presence of a catalyst with or without a radiation source to generate highly reactive radical specie capable of degrading organic pollutants in wastewater	Functional in gaseous process Fast action Does not produce toxins in water Efficient colour reduction in waste water at a low dosage Highly susceptible to many factors	Very little half-life Generates poisonous and carcinogenic aromatic compounds Very costly High instability of oxidizing agents	[154,155]
	Photochemical processes of electrochemical destruction	It involves the UV treatment of wastewater laden with dyes in the presence of H2O2 to breakdown the dye molecules into smaller organic molecules or for complete degradation into products such as CO2& H2O, other inorganic oxides etc.	Efficient for wastewater decolorization Little or no sludge generation.	Possibility of formation of Toxic by-products	Sioni, 2017
	UV-peroxide system cucurbituril Sodium hypochlorite Treatment		Effective for cleaving azo linkages	Formation of mutagenic by-products Releasees toxic chlorine gas	[154]
Biological	Biosorption	biosorption entails passive dye uptake by dead microbial cells	It is cost-efficient May be selective	It is a slow process Inefficient for persistent dyes	[148]
	Bioaccumulation	This is the dye uptake by living microbial cells.	Cost-effective Selective	Not advisable for continuous process Ineffective for recalcitrant dyes	Buruna et al., 2013 [55]

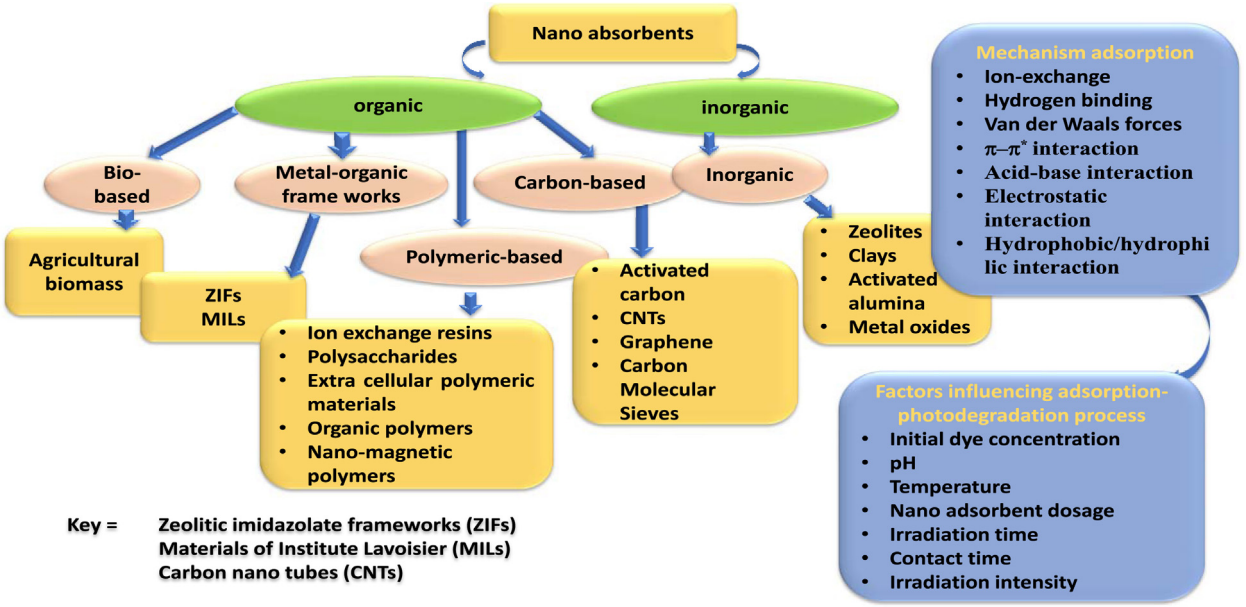

Fig. 5. Categories of nano-adsorbent, mechanism and parameters influencing their performance.

studies have emphasized the use of adsorption and biological treatment process which are classed as secondary treatments given to textile wastewater. However, the problem of disposal of sludge and the recovery of materials used for the treatment process are fundamental challenges of these technologies [85,111]. On the other hand, the use of advanced oxidation processes in recent times has appreciable advantages of faster reaction kinetics and the generation of little or no toxic sludge. However, the sophistication of some instruments for the treatment brought about the study of high dye remediating photocatalysts using which gives provision for the use of various nanomaterials in their pure form and as composites with the possibility of recovery [45,106]. These evolving limitations gave rise to the evolution of the photocatalytic treatment approach for textile wastewater using nano polymeric composites (Jangid et al. [181]).

Nano technology in photocatalysis

The uses of nano technological materials as adsorbents have grain prominence and applicability to environmental science. This thematic field studies the use of nano scale materials (10^{-9}) characterized by novel, versatile and multiple functionalized properties for the treatment of toxic dye pollutants [17]. The transition in structural, functional and reactivity of nanomaterials from bulk scale to nano-size offers its desirable usage as a catalyst in photocatalysis [37], Mishra [75]. Although, these materials are generally classed as conductors, semiconductors and insulators. However, this classification is a function of the value of their respective bandgap, which is pivotal for the photocatalytic process [8,130]. Nano adsorbent materials are broadly referred to as either organic or inorganic (Fig. 4) with distinguishing features of photosensitivity, high surface area, high thermal chemical and mechanical stability, appreciable electrostatic features, compressibility, tunability of pore volume and bandgap, high magnetic and adsorptive capacity and enhanced solubility properties due to short intra-particle diffusion [36,124].

These distinguishing features account for their application in the photocatalysis of recalcitrant dye molecules in industrial effluents [13]. The use of the photocatalytic technique in nanotechnology is described as a photon-induced molecular transformation that occurs at the surface of exciting photoactive nanomaterial adsorbing organic pollutants (e.g dye molecules) from the wastewater [86]. The mechanism of the degradation process starts with the capturing of photon energy from light by the photocatalyst leading to the excitation of the electrons from the valence band (VB) to the conduction band (CB), forming oxidizing and reducing sites (Fig. 6) (Antonio et al., 2019) [86]. For electronic excitation to occur, the energy of the photon captured by the material must be equal to or greater than the energy of its bandgap. This excitation leads to the generation of hydroxyl radicals (•OH), superoxide radical anions ($\bullet O^{2-}$), and hydroperoxyl radicals (•OOH), which are oxidizing species (Xing et al., 2018). Dyes adsorbed already by the nano adsorbents from the wastewater combine with the electrons in the conduction band resulting in the formation of dye radical anions and consequently degradation of the dye molecules (Hossain et al. [205]; Sioni et al., 2020). For instance, in the photodegradation process of azo dyes present in textile wastewater, the energy of photons captured via UV or sunlight generates electron-hole pairs (e^- and h^+) which migrate to the surface and site of the adsorbed azo dyes.

This migration set-up a redox reaction (Fig. 6), which produces oxidizing radicals that attacks the adsorbed azo dye molecules and degrade them into non-toxic substances such as H_2O *and* CO_2 (Comparelli et al. [182]; Zhu et al. [183] 2013;

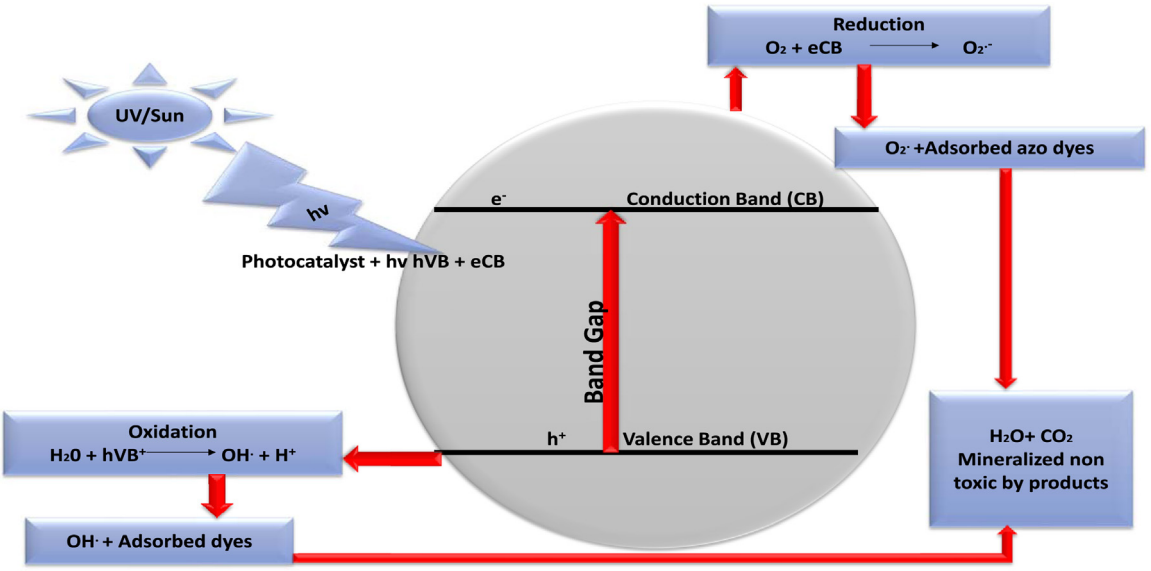

Fig. 6. Mechanism of Azo dye degradation in photocatalysis.

Soltani and Entezari [184]; Ullah et al. [185]). Photocatalyst nano-adsorbents used for this process can be bio-based, metal-organic frameworks (MOFs), carbon-based, polymeric-based or inorganic as described in Fig. 4 However, commonly used nano adsorbents in photocatalysis are the inorganic metal oxides (Table 3) [85]. This is due to the promising potentials such as photon detection and capturing, electronic structure, carrier transportation and band gap [30,77,110].

The study by Dutta et al. (2021) reveals that metal-oxides-based adsorbents exist as magnetic or non-magnetic. An investigative study by Mohamed et al. [79] on one of the magnetic classes of the nano-adsorbents (Fe3O4-Nps) has an adsorption capacity of 150–600 mg g^{-1} for rhodamine dye within 30 min, while the fabricated composites such as Fe_3O_4/CeO_2, Fe_2O_3–Al_2O_3 have a notable adsorption capacity of six-times higher than the pure metal oxides nanomaterial in dye remediation [73]. This action is due to their surface-to-volume ratio and pore size, which is consequent to bandgap tuneability for improved photocatalytic effect [33,36,112,132]. On the other hand, the non-magnetic metal-based oxides ZnO, TiO_2, MgO are often fabricated as a hybridized composite with notable adsorption efficiency [36,85].

Examples of these composites with their corresponding adsorption capacity include Co/Cr-co doped ZnO with 1057.9 mg g^{-1} for methyl orange, ZnO–Al_2O_3 nano adsorbents for Congo red and Ni-MgO having maximum adsorption of 397 mg g^{-1} [62,64,79]. Dutta et al. (2021) revealed that apart from their appreciable specific surface area, the charge on the adsorbent surface gives room for electrostatic dye-adsorbent interaction. Also, the polymorphic nature of the composite nano adsorbent creates a more active site for the binding of dye molecules. Although the challenges of toxicity and frequent recombination notably exist for the metal oxides photocatalyst in Table 4 ,which greatly limits their performance in dye degradation [8,42]. Additionally, ceramic nanoparticles are another class of adsorbent chemically existing as oxide, phosphate and carbonates (silica, alumina, titania, zirconia), with high chemical inertness and heat-resistance [36,58]. However, the limitation of the large bandgap of these materials incited the study of carbon-based nanomaterials with unique structural features fit for adsorption and composite fabrication. Carbon-based nanomaterials generally exist as either carbon-nanotubes (single-walled or double-walled) or carbon-fullerenes [103]. One of the unique examples of carbon-nanotubes (CNTs) is graphene sheet which can be rolled in the form of tubes, having characteristic features of thermally-conductive, less toxic photoactive, bandgap tunability and synergistic composite forming potential [38,42,131].

Bezerra de Araujo et al. [18], Oni and Sanni [88] and Sivakumar et al. [121]discussed the high adsorptive performance of GO for toxic dye pollutants such as Direct Red 81 and Indosol SFGL direct blue, crystal violet and methyl orange, and methylene blue respectively at pH 6-7. Sivakumar et al. [121] added that the efficiency of GO is due to the interaction of the hydroxyl and carboxylic groups with the auxochormic substituents (functional groups) on the dye molecules. Furthermore, Zheng et al. [140] related that the hierarchically unique orientation of GO–NiFe-LDH nano composites enhance its adsorption efficiency for Congo red and methyl orange at 489 and 438 mg/g respectively. Similarly, the composite of GO with metal oxides (GO/MgO) studied by Heidarizad and Şengör [49]notable adsorption of 833 mg/l within a contact time of 60 based on the multiple functional sites available for binding. Although GO is thermally, mechanically and chemically stable, however, the need for the use of photosensitizers in place of toxic metal and metal oxide NPs justifies the investigation of p-type conductive polymers especially the novel polyaniline and its composite forming mechanism with other materials with appreciable advantage

The beneficial attributes of high effective surface area, high selectivity and absorptivity, appreciable doping/de-doping technique, effective electrical transport characteristics, well-established binding affinities, and unique textural properties of-

Table 3
Operational parameters for adsorption-photodegradation process.

S/N	Parameters	Description	Effects	Ref.
1	pH	The measure of the degree of acidity or alkalinity of the medium. The variation of measured pH is a function of the acidic or basic constituent of the medium	Influences adsorption-desorption of dyes molecules on the surface of the photocatalyst Affects the rate of generation of the photoactive radicals Determines stability of nano adsorbent Influences attraction of nano materials and water molecules Low and high pH enhances anionic and cationic dyes respectively Influences ionization level and adsorbent surface charge of the adsorbent Determines the size of catalyst aggregates alongside the positions of the valence band and conduction band.	[26,36,98,117]
2	Temperature	The degree of hotness or coldness on a chosen scale. It describes the nature of the process whether endothermic or exothermic.	Increasing temperature increases the adsorption and dye degradation rate due to increased activation energy below 80 °C Increasing temperature decreases the solubility of dye and increases its adsorption. At temperature above 80 °C, recombination of electron-hole pair of the nano adsorbent sets and reduction in adsorption of dye molecules. Increasing temperature increases the system entropy which enhances the surface activity	[26,36,60,81]
3	Nature and dosage of nano adsorbent	It describes the functional, structural and molecular constituents of the nano composite and the amount in wt/wt% applied for the adsorption-degradation process.	Determines the bandgap of the adsorbent which influences its photoactivity Influences material crystallinity, possible agglomeration and decrease in surface area Determines the dye-adsorbent contact angle Increased dosage beyond the optimal point reduces the adsorption capacity due to site congestion Determines the adsorption-desorption equilibrium	[26,57,68]
4	Initial concertation of dyes	This is the amount of dye molecules initially present in the effluent or available for binding onto the nano adsorbent.	It determines the equilibrium phenomena existing between the solid-liquid phase of the active sites and the dye molecules A high concentration of the dyes molecules lowers the adsorption and consequently reduces the photodegradation due to site saturation of the active site	[26,36,50]
5	contact time	This is the duration required to establish adsorption-desorption equilibrium	Low contact reduced the adsorbed dye molecules and at higher contact time beyond the optimal duration, saturation and desorption set in. High contact time comes with a higher energy requirement for the processes	[36,126]
6	Irradiation time	This involves the time with which the adsorbent-adsorbate at equilibrium is exposed to photon energy from UV or sunlight (visible)	Determine the rate and extent of photodegradation Higher irradiation time requires higher energy	[81,117]
7	Irradiation source intensity	This describes the origin of the photon energy captured by the photocatalyst which could be from UV or sunlight and the degree of intensity of light incident on the system	The photonic nature (UV or sunlight) determines the excitation of the photocatalyst and the performance in dye degradation Degradation increases with increasing photon intensity Determines the photon-generated electron-hole pair during excitation and the kinetics of the rection	[26]

fer polyaniline a leading advantage [71,118]. Mu et al. [84] reported a high adsorption capacity of 248.76 mg g^{-1} for Congo red dye graphene/polyaniline and PANI/Fe3O4 respectively. Although in its purest form Smita et al. [122] reveal that PANI exhibit an adsorption efficiency of 92% for methyl orange due to the structural versatility and the presence of amine and imine active group. However, higher adsorption and reduced recombination enhance photodegradation when hybridized composites of PANI are formed with other nanomaterials [103]. This also improves the surface area and enhances photocatalytic reaction sites thereby inducing electron-hole separation [92]

Operational parameters for adsorption-photodegradation

In photocatalysis, vital parameters such as pH, initial dye concentration, temperature, nature and dosage of nano adsorbent, contact time, irradiation time, and irradiation intensity play a significant role in the adsorption-degradation process as described in Table 3 [15,93,96]. As the initial dye concentration increases the adsorption and degradation increase up to the point where the binding sites on the adsorbent are saturated, beyond this point desorption occurs [35,93,99]. The pH on the other hand plays a very crucial role in the determination of adsorption and consequent degradation of dye molecules ad-

Table 4
Physical properties of conventional photocatalyst Nano- absorbent.

S/N	Photocatalyst	Properties	Advantages	Draw backs	Ref.
1	TiO2-Nps	Exists as anatase (tetragonal), Rutile (tetragonal) and Brookite (orthorhombic) 3.0–4.123 eV The particle size of 10–50 nm The surface area of 98.2 m^2/g for pure nano-powder	Low cost Most effective Non-toxic High stability against photo corrosion	Large band gap Inability to operate with visible light Rapid electron-hole recombination Little or no possibility of recovery and reuse Responds only to UV light Non-porous in nature Challenges of agglomeration and aggregation low quantum efficiency photo-corrosion	[117,120]
2	ZnO2-Nps	Rod-like, star-like and isometric 3.3 eV band gap 14–32 nm The surface area of 88.89 m^2/g for pure nano-powder	Low cost Low toxicity Ability to absorb a larger fraction of UV-spectrum	Inability to operate with visible light Challenges with photo corrosion in water Little or no possibility of recycling and reuse	[97,125]
3	Fe2O3-Nps	has rhombohedral, corundum, cubic or body centred 10–40 nm The surface area of 30.71 m^2/g – 93.84 m^2/g 2.3 ev band gap	Unique stability Possibility of recycling and reuse abundance in the earth	Low diffusion length Challenges of high electron-hole recombination rate Unsuitable for the aqueous phase due to its hydrophobicity Possibility of agglomeration and clump formation Increased particle size due to high surface energy	[51,113]
4	WO3-Nps	Nano tubular structure 2.4–2.8 eV bang gap 12- 85 nm 11.173-11.705 m^2/g surface area	Ability to respond to both UV- and visible light	The stability of triclinic WO3 is only at low temperatures (>17 °C) Its efficacy is only in acid-catalysed reaction Rapid recombination of electro-hole pairs	[23,28,78]
6	Graphene Oxide (GO)	2D micro-sized planar sheets 3.97–4.08 eV 30–200 nm The surface area of (±1292) m^2/g	High photosensitizing potential more to its more positive Fermi level forestalls frequent electron-hole recombination low toxicity large theoretical specific surface area and tuneable bandgap, High electron mobility and thermal stability High mechanical strength	Require great handling and improved surface properties during synthesis.	[42]
7	CdS-Nps	Disk/core-like structure 1.7–2.4 eV 47–73 nm The surface area of 7.89 and 10.26 m^2/g	Ability to capture photon energy with the visible and UV region Unique optoelectronic features Electron-hole recombination challenges Chemical and thermal stability	Low stability in solution Requires combination for better charge extraction Low specific surface area Fast recombination rate of electron-hole pair Easy agglomeration Toxic	[52,91]
8	SiO2 Nps	Spherical shape 15 ± 8 nm 2.5-2.8 eV The surface area of 47.0- 289 m2/g.	Low absorption in the UV region however appreciable absorption in the visible region dielectric electrons low toxicity high surface area high adsorption capacity	Low photon capturing potential	[12]
9	PbS-NPs	face-centred cubic lattice 0.286–0.5 eV 40–70 nm	Effective in visible light region Excellent photon detector.	Frequent electron hole-recombination Toxic agglomeration and recombination	[76]

(*continued on next page*)

Table 4 (*continued*)

S/N	Photocatalyst	Properties	Advantages	Draw backs	Ref.
10	PbSe-Nps	Cubic-like structure 0.165–0.27 eV 10-30nm The surface area of 0.7–1 m2/g	Appreciable thermal stability Excellent photon capturing potential Good optoelectronic properties	Frequent electron hole-recombination Toxic agglomeration and recombination	[32]
11	Cu2O-NPs	500 nm–100nm 2.172–2.4 eV The surface area of 3.3 and 1.3 m2/g	Possibility of reusability High photon capturing ability High thermal stability	Challenges of electron-hole recombination Possibility of photo corrosion	[94]
12	ZnS	Polymorphus nano material 3.6–3.7 eV 25–40 nm Surface area of 0.3 to 68 m^2/g.	Excellent photon trapping effect Rapid generation of carriers Excellent chemical stability	Stable at low temperature Limited to visible light absorption Frequent recombination of electron-hole pairs	[8]
13	CdSe-Nps	A spherical monodispersed particle 4.5–9.7 nm 1.7–2.0 eV	Active under visible light Appreciable photon capturing potential	The problem of electron-hole recombination Toxic	[96]
14	SnO2-Nps	Spherical shape 3.54–3.8 eV 9.5–10.5 nm The surface area of 47.8574 m^2/g	Appreciable luminesce and photon capturing potential High chemical stability Good optoelectronic properties	The problem of electron-hole recombination Acute toxicity	[37]
15	Ag-Nps	Spherical morphology 5–10 nm 1.75–2.75 eV The surface area of 23.81 m2/g,	Appreciable photon capturing potential Environmentally friendly Cost-effective via biosynthesis high stability ability to capture photon energy from the visible region	Problem of agglomeration Challenges of photo-corrosion	[40]
16	CdO-Nps	Structurally exist as tubes, rods and cauliflower-like 8.8 nm 2.2–2.5 eV 118–143 m2/g	Respond to both UV- and visible light Very effective for especially basic dyes Well-ordered crystalline pattern	Possibility of recombination of electron-hole pair Toxic	[117]
17	CuO-Nps	Monoclinic structure 200–500 nm 1.21–1.5 eV The surface area of 0.761 and 0.299 cm3·g−1	ability to perform under irradiation in sunlight effective for alkaline photo-decolorization High adsorption capacity and exceptional uniformity in the pores Unique ion-exchange ability Cost-effective	Frequent electron-hole recombination Possibility of photo corrosion Limitations based on agglomeration	[94]
18	ZrO2-Nps	Polymorphic in nature 5.0 eV 11–78 nm The surface area of 25–85 m^2/g	Non-toxic Chemical stability Appreciable hydrophilicity Cost-effective Excellent optoelectronic properties	Frequent electron-hole recombination Conductivity is temperature sensitive	[15]
19	In2O3-Nps	Polymorphic in nature 8–9 nm The surface area of 38.1 m2/g 3.5–3.7 eV	High conductivity Excellent photochemical stability Ease of surface tunability Good dispersion property Posses anti photo corrosion activity Effective photon sensitizer from UV to visible	Frequent electron-hole recombination Toxic	[138]

(*continued on next page*)

Table 4 (*continued*)

S/N	Photocatalyst	Properties	Advantages	Draw backs	Ref.
20	Nb2O5-Nps	Orthorhombic nano fibers 3.4–3.6 eV *4.5* nm Surface area97.5 m2/g	High stability in aqueous medium Appreciable surface acidity, redox photocatalytic properties High adsorptive capacity Good chemical stability	Frequent electron-hole recombination Toxic	[67,85]
21	h-2DBN	Sheet-like in structure 5–6 eV 114 nm The surface area of 19.04 m2/g	high thermal and chemical stability improves Visible light absorption forestall recombination of electron-hole pair appreciable visible light response forestalls frequent electron-hole recombination	Low photosensitizing potential	[112]
22	V2O5	Spherical morphology 2.3–2.52 eV 10nm	High chemical stability appreciable visible light response tuneable surface morphology high resistance to photo-corrosion	Frequent electron-hole recombination	[24]
23	Sn3O4	Flower-like structure 2.5–2.9 eV	Ability to use photon energy from sunlight and UV High adsorption capacity Appreciable optoelectrical properties	Frequent electron-hole recombination	[53]

sorbed onto the surface of a nano photocatalyst [95]. Research by Salleh et al. [104] reveals that low and high pH enhances the adsorption of anionic and cationic dyes, respectively. This claim was affirmed by Daneshvar et al. [29] and Phoemphoonthanyakit et al. [89] in their research where higher adsorption of 1093 mg g^{-1} at pH 2 for Acid Blue 25 and 600 mg g^{-1} at pH 7 for Rhodamine 6G at pH of 2 and 7 respectively.

Furthermore, photocatalytic decomposition of dye molecules in wastewater has been studied at pH values ranging from 3 (acidic) to 13 (alkaline) for anionic, cationic and neutral dyes in wastewater [69]. The pH value required for the reaction is suggestive of the kind of charge on the surface of the nano adsorbent. This is because at pH <pHzpc, pH>pHzpcor pH=pHzpc it implies that the surface charge is positive, negative and neutral respectively [15]. Hence, cationic dyes are adsorbed more in an alkaline medium to establish electrostatic interaction resulting in increased degradation efficiency [15,53]. Alakhras et al., [5] added that at low pH there is a notable reduction in the production of hydroxyl radicals by the positively charged surface which is needful for hydroxyl radical formation. Also, temperature requirement quantitatively determines whether the process is endothermic or exothermic which influences the adsorbent-adsorbate interaction prior to photocatalysis [35].

Physical properties of nano-adsorbent used in photocatalysis

Generally, physical properties such as high selectivity, high absorption capacity, durability, reusability, cost-effectiveness, surface area, optoelectrical properties, crystallite size and distribution, dispersibility, and mechanical and thermal stability are vital properties that determine the choice of nano adsorbents materials in photocatalysis [41,42]. Table 4 describes the physical properties of the commonly used conventional catalyst with metal oxides taking the highest frequency of use [37]. Although the frequent use of these is based on their polymorphic nature. However, electron (e^-)- hole (h^+) recombination, agglomeration and photo-corrosion of some of the metal oxide nanoparticles limits their performance, recovery and reuse (Meng et al. [186]). Another limiting challenge of this conventional catalyst is that their photo capturing propensity is only within the ultraviolent region Beyond this region to the visible, the nanomaterials exhibit low photon detection and capturing potential which lowers the generation of radical species needful for dye degradation [25]. Furthermore, from Table 4, semiconductors such as TiO_2,h-2DBN, Nb_2O_5, ZrO_2, and ZnO2 have appreciably high band-gap which limits their photon capturing potentials, especially when irradiated within the visible region [112,130]. Additionally, the use of these semiconductors in their pure form as nano-adsorbent has toxicological impacts and reduced photocatalytic performance [13,136]. Xu et al. [187] suggest that the reduction in adsorption capacity during adsorbent-adsorbate contact is due to the saturation of the adsorbent surface and charges present on synthetic dye molecules, especially azo dyes. For instance, cationic azo dyes easily undergo adsorption and degradation when compared to the anionic azo dyes such as Eriochrome Black T due to the lack of electrostatic interaction [74] (Xu et al. [187]). This is due to the charge present on the nano-adsorbent, the difference in sorption mechanisms and the value of the pH which is greater than the pHpzc, favouring the preferential adsorption of cationic dyes compared to its anionic counterpart [15,116]. This action justifies the report on the faster adsorption-degradation kinetics of cationic azo dye using TiO_2 when compared to the anionic quinizarin, having a low adsorption efficiency of 21.8% with the same catalyst (Abuabara et al. [188]; Pereira et al. [189]).

Also, the challenges of recovery and reuse of conventional catalyst after the process of photocatalysis has limited their commercial acceptance in the treatment of wastewater laden with recalcitrant dyes from textile industries (Muhd et al. [190]). Hence, tackling the attendant limitations of these nano-adsorbent requires the fabrication of nanocomposite by combining these semiconductors with a photon sensitizing conducting polymer (PANI) characterized by high resistance to corrosion, high adsorptive capacity, chemical and thermal stability and versatile surface area [54,112]. The fabrication of composite mix form using these materials enhances surface modification and bandgap tunability necessary for improved performance (lowering the bandgap- Fig. 7) [30,112].

Synthesis and unique novelty of polyaniline in photocatalysis

There are various types of π-conjugated conducting polymers with appreciable conductivity and novelty. These emerging conducting polymers include polyaniline (PANI), polythiophene (PTH), polypyrrole (PPY) poly(para-phenylene) (PPP), poly(phenylenevinylene) (PPV) and polyfuran (PF) [17,22,44]. However, the most prevalent among these varieties is polyaniline (PANI). This is based on unique properties such as exceptional electronic and optoelectronic features, cost-effectiveness, ease of synthesis, environmental stability, high electrical conductivity, high thermal power and unique structural ordering [19,65,87,110]. Various approaches such as interfacial polymerization, seeding polymerization, vapor phase self-assembling polymerization, photo-induced polymerization, plasma polymerization, sonochemical synthesis, and electrochemical synthesis can be used in the synthesis of polyaniline [19,109]. However, the solution technique via oxidative polymerization of aniline with ammonium persulphate is commonly used due to its faster polymerization rate and excellent yield (Fig. 7). The resultant products of this polymerization process can be either leucoemeraldine (fully reduced state), emeraldine salt (half oxidized state) or pernigraniline (fully oxidized state) which are described in Fig. 7 [17,19]. Out of these products, emeraldine salt stands out with unique structural characteristics of two benzoid units and one alternating quinoid unit which results in high thermal stability and nanocomposite forming potential with inorganic nanoparticles such as CeO_2, TiO_2, ZrO_2, Fe_2O_3, Fe_3O_4, ZnO and TiO_2 thereby generating nanostructures such as nanofibers, nano tubes, nano sphere and nano flowers [17,19]

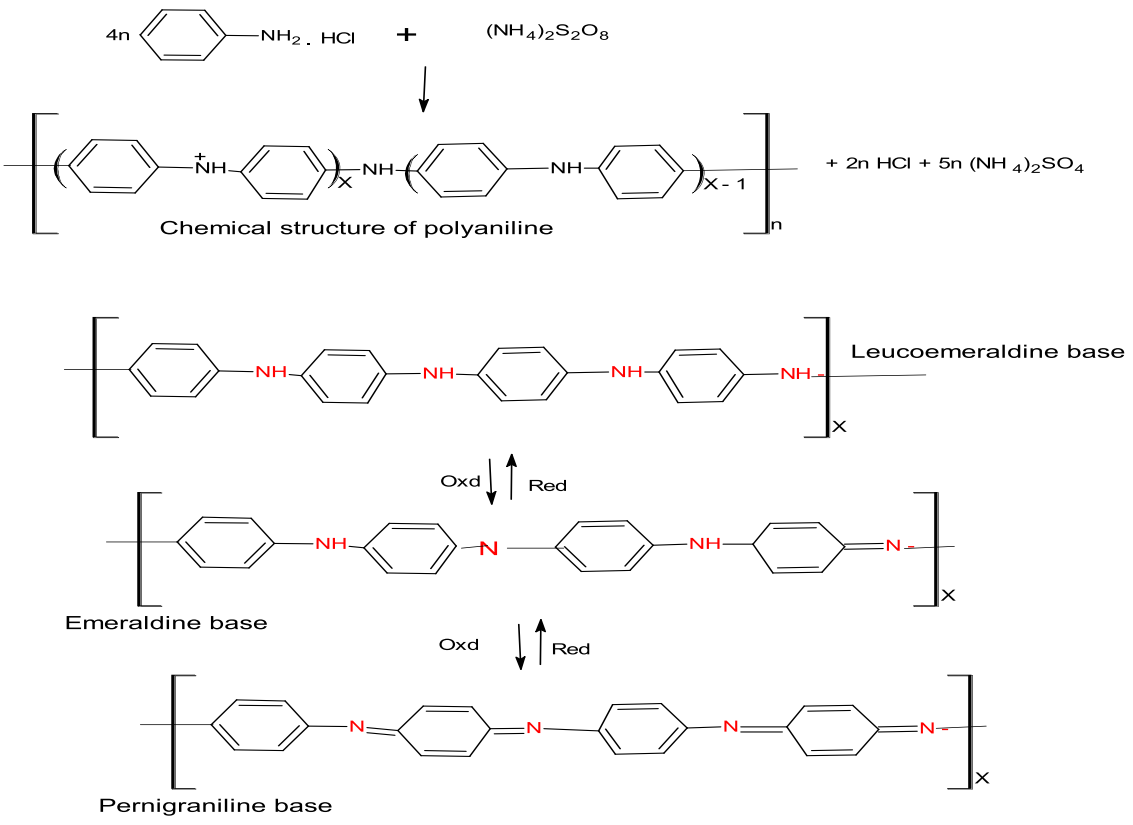

Fig. 7. Oxidative polymerization of polyaniline into chemical forms.

These unique structural features and versatility account for its vast application in corrosion protective coatings, energy devices, sensors, water purification and as photocatalyst [100,111]. Current research reveals that PANI exhibits incredible photoelectronic properties and the composite resulting from its incorporation with other materials has appreciable synergic properties higher than the use of polymers [87,109,137]. Furthermore, PANI is amphiphilic based on its conjugated organic part (Quiniond) and–$NH^{\bullet+}$ formed during protonation, the excellent dispersion and ability to bind with organic and water-soluble dyes in effluent account for its choice among other polymeric adsorbents [19,20,66,141]. Also, the structural ordering of the polymer chain and its high conjugation give it dynamic electrical properties associated with high carrier transport mechanism which is vital for the photocatalytic process [19,109]. The dynamics of electrical transport in polyaniline are described by its intra-chain or inter-chain transport processes [109]. The inter-chain transport process depends on the carrier delocalization of the polymer chain with appreciable conjugation length [63]. On the other hand, the inter-chain charge transport process is dependent on the hopping mechanism, based on the molecular crystalline packing of the polymer matrix [30,109]. The unique molecular orientation of PANI accounts for its improved charge mobility properties which enhances its photosensitivity when existing in pure form or as composites with other semiconductor materials [83]. Apart from the hopping of charge carriers along and between polymer chains, other incredible conductive mechanisms of polyaniline can be tunnelling between high-conductive crystallites embedded into the amorphous matrix or electron-phonon interaction [30].

Mechanism of composite fabrication and dye-photocatalyst interaction

Composite fabricated from PANI is aimed at tackling the inefficiency of conventional catalyst and treatment process for recalcitrant dyes. Various cost-effective and environmentally friendly approaches have been investigated by literature on the fabrication of polymeric nanocomposite catalysts with polyaniline (Liu et al. [204]). Studies show that the fabrication of these novel nanocomposites is mostly by ex situ or *in situ* polymerization (Vargas et al. [191]). The ex-situ polymerization involves the mixing under sonication of the semiconductor's particles with already synthesized polyaniline (Cruz et al., 2017). However, the commonly used composite fabrication technique (*in situ* polymerization) involves homogenous dispersion of the nano-grade semiconductors or other nano-size materials of choice during the polymerization process of polyaniline (Fig. 8). This method of fabricating nanocomposite is more appreciable than the former because the former exhibits the formation of low-density and non-uniform coverage of nanostructures of polyaniline by the material semi-conductor (Vargas et al. [191]).

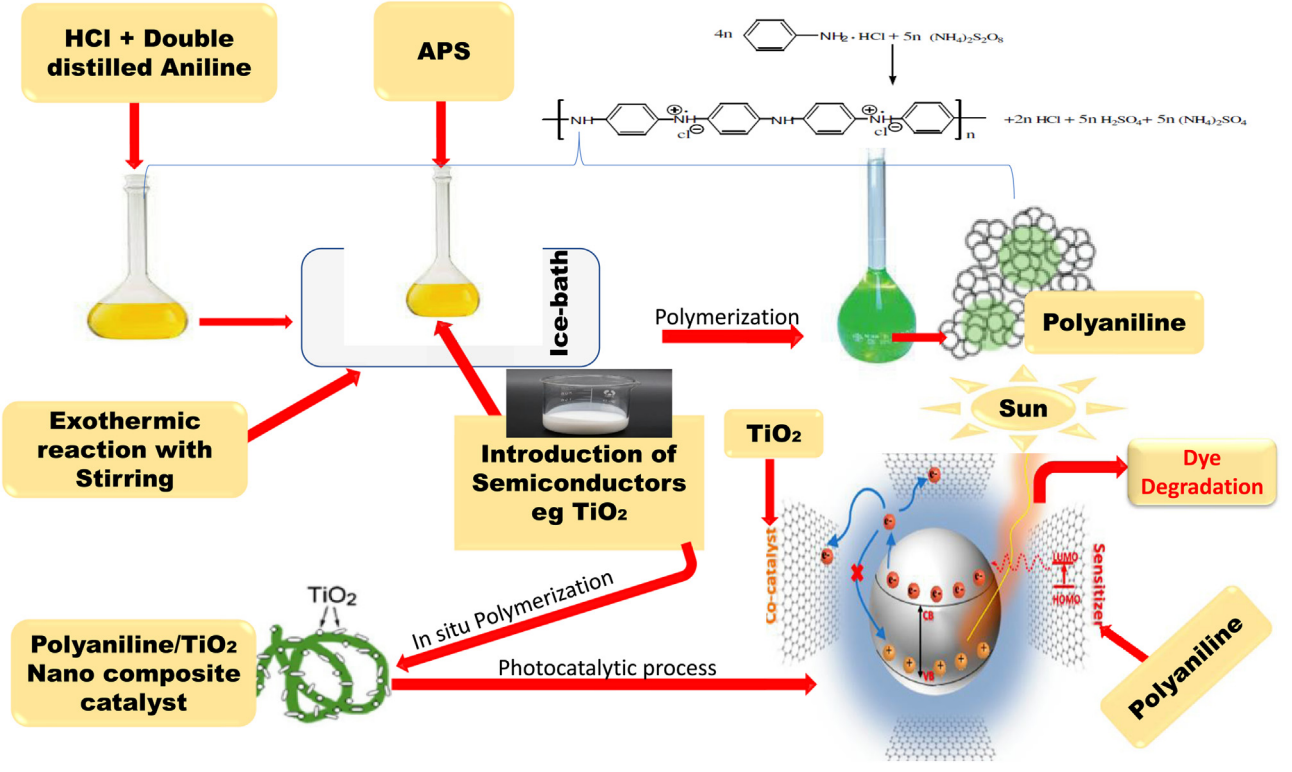

Fig. 8. Pathway of Synthesis, composite fabrication and degradation of dyes by the nano composite of PANI.

The *in-situ* polymerization of polyaniline with semiconducting material such as TiO_2, ZnO_2, forms coupled nano polymeric composites (Figs. 8 and 9) (Tai et al. [192]; Liu et al. [204])

During composite fabrication, PANI acts as a photosensitizer while interacting with the bandgap of the semi-conductors in Fig. 9. This consequently lowers the bandgap of the The presence of the semiconductor provides the composite with appreciable morphological structure for dye adsorption [101]; Jangid [181]). Consequently, composite mix improved the subsequent performance of the photocatalyst by preventing frequent recombination of electron-hole pairs during photocatalysis (Jangid [181]). Furthermore, during photocatalysis, the advantages of high mobility charge carriers, stability, and the strong coupling effect existing between the polymer and the semiconductors, make the nanocomposites function effectively in the degradation of dye molecules within the visible region. (Bingham and Daoud [193]; Riaz et al. [99]; Jadoun et al. [194]). Ansari et al. [195] and Hao et al. [196] added that the tuned morphological property of the composite proffer higher performance in photocatalysis compared to the conventional catalyst. Morphologically, the presence of PANI enhances the high hole transporting ability and stability of the material during the remediation process (Vikas et al. [197]). Jangid [181] and Shahabuddin et al. [112] revealed that the presence of the conducting polymer in the composite mix accounts for the photocatalytic stability and activeness of the material under visible light after five consecutive runs. Studies by Saha et al. [101], Shahabuddin et al. [112] and Ameen et al. [10] reveal that PANI exhibited well-defined tubular morphology, however, incorporation of h-BN and graphene nanosheet correspond to the formation of the granular polymeric network. Consequently, the surface modification improved the adsorption capacity by enhancing the availability of the binding sites of the composite for adsorption [39,101]. Furthermore, in Fig. 9, the adsorption of dye molecules unto the surface of the nano composite of polyaniline is higher as a result of electrostatic interactions and $\pi-\pi^*$ conjugation among the aromatic rings of dye molecules [109,110]. In the fabricated composite, PANI act as a photosensitizer via photon capturing and excitation of valence electrons in HOMO, jumping to LUMO through $\pi-\pi^*$ transitions [19,76,112]. Also, the incorporation of semiconductor material into the PANI polymeric chains by *in situ* polymerization prevents recombination such that, as the positively charged holes (h^+) are returning to HOMO to recombine, the empty conduction band of the semiconductor intercepts the recombination thereby improving it photocatalytic efficiency [8,42,112].

Improved functional properties of polyaniline-based nanocomposites: current scope

The current research scope focuses on the vital need to improve composite fabricated from polyaniline to enhance effective industrial performance, recovery and reuse [85,120,135]. Recent studies discussed the use of immobilization techniques to enhance the recovery and improve the performance of these catalysts for several runs [97,120]. The study suggested the fabrication of nano composite photocatalyst via immobilization of the semiconductors either on the surface or in the PANI polymer matrix [117]. The technology involving the immobilization of the photocatalyst nanoparticle on the surface of the polymer matrix could be via dip-coating, chemical vapour deposition, grafting or plasma treatment followed by UV irradiation (Fig. 10) [7,21,66,135].

Alhaji et al. [7] and Lin et al. [66] added that this method enhances the reduction of agglomeration, creation of more active sites, surface modification and its cost-effectiveness. Although the method is disadvantaged by wide particle size distribution. On the other hand, the technology involving the immobilization in the support matrix enhances the reduction in leaching at lower energy and higher catalyst recovery propensity, although may be limited by agglomeration inside the matrix [117,135]. One of the most effective processes in immobilization in the polymer matrix is the in-situ process. This process is characterized by considerable advantages of lower bandgap and higher dye-degrading efficiency as highlighted in Table 5. The in-situ process can either be by *in situ* polymerization (described in Fig. 8: incorporation of TiO2 on PANI nano rods), or the sol-gel method [54].

The in-situ polymerization involves a controlled blending of selected semiconductor nano material with the neat monomer before subsequent polymerization [117]. However, the sol-gel approach is a two-stage technique that involves hydrolysis where bond cleavage occurs between the organic matrix and the semiconductor nano powder before condensation which involves bond formation alongside small leaving groups [3,34]. The use of the in-situ process enhances the homogenous dispersion of the semiconductors on the PANI matrix, and reduces possible agglomeration [3,34]. Examples of other processes are mixing, hydrothermal method catalyst deposition, galvanostatic method and plasma-irradiation treatment which have the challenges of nano powder agglomeration and its energy-intensive [46]. Studies carried out by Jangid et al. [54] and Shahabuddin et al. [112] on the fabrication of catalyst nano composite via *in situ* polymerization to generate hybridized h-BN/PANI and TiO2/PANI nano rod exhibited excellent photodegradation efficiency of more than 90% and with over four runs due to the immobilization of the nano powder in the polymer matrix which enhances the recovery and reuse. Similarly, Mondal & Sharma [81] and Singh et al. [119] also suggested the use of the immobilization method in the polymer matrix to improve the adsorption capacity enhance their photocatalytic water splitting potential and boost the possibility of recovery of titania.

Also, Lin et al. [66] discussed three possible approaches to improve the functional features of the polyaniline-based nanocomposite. Firstly, the solute-solvent interaction of PANI can be enhanced via the use of Graphene oxides (GO), and CNTs as additives which limit fouling, enhance the rate of flux recovery and improve the hydrophilicity of the conducting polymer. Secondly, the use of secondary amine with molecular width < 4.53 Å and a pKa>7 to facilitate gelation inhibition. This also provides needful solvent-polyaniline interaction for the enhanced adsorptive potential of the nanocomposite. Thirdly, the use of zwitterions to form zwitterionic polyaniline. The zwitterions are characterized by charge functional groups

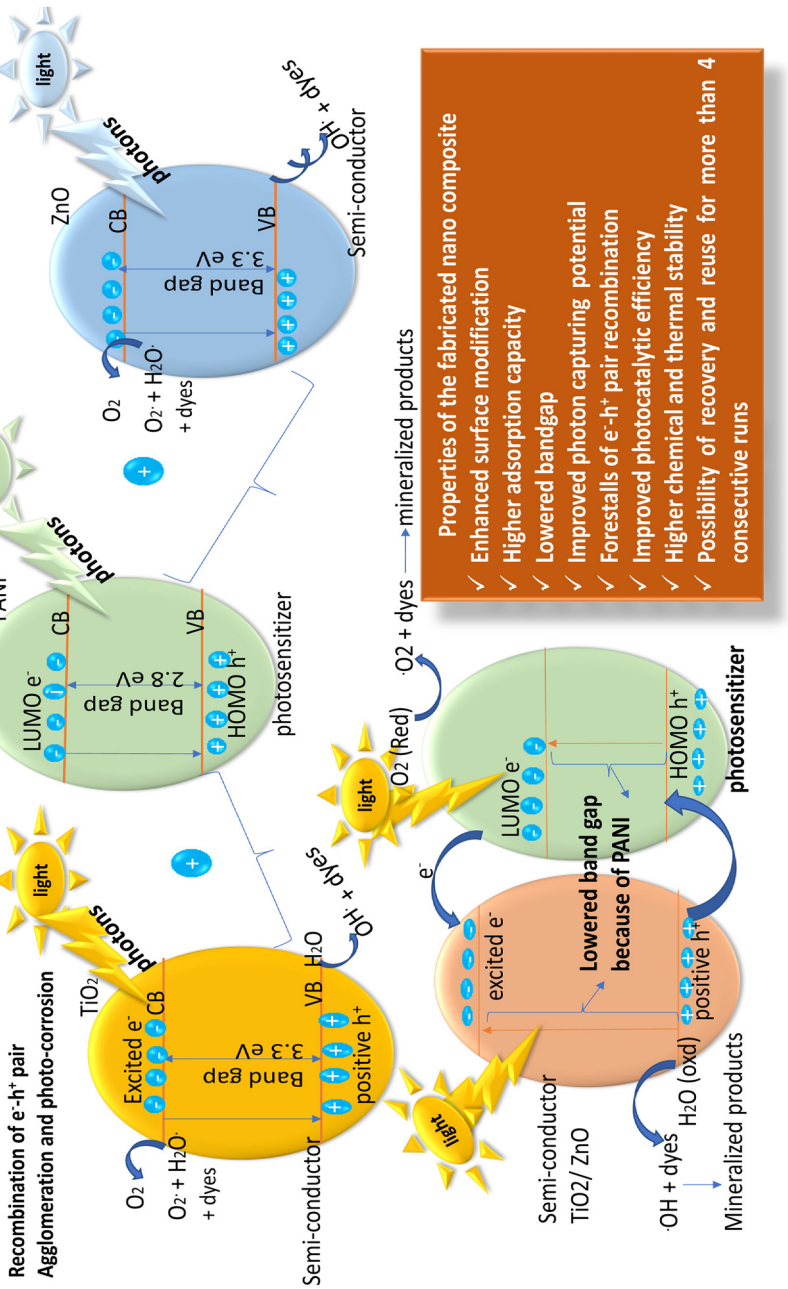

Fig. 9. Mechanism of dye interaction with pure semiconductors and PANI/TiO_2 nanocomposite.

Table 5
Immobilization techniques and tuned bandgap values of photocatalyst composites.

S/N	Photocatalyst	Immobilization techniques	Operating conditions							Ref.
			Initial conc (mg/L)	pH	Catalyst dosage (g/L)	Irradiation time (min)	Light source (W/m^2) or W	% Degradation	Band gap (eV)	
1	PANI/TiO2	Mixing	5.0	-	1.2	360	Visible 610.3	99	3.10	[61]
		In situ polymerization	10	10	1.2	70	UV 350	90	3.10	[139]
2	PANI/ZnO2	Mixing	10	7	1.5	180	UV 31	98.3	2.67	[108]
		In situ polymerization	10	7	1.5	180	Visible 250W	97	2.81	[11]
3	Cu2O-ZnO/PANI	*In situ* polymerization	30	6	0.05	30	Visible 100W	95	2.68	[80]
4	FeO-ZnO/PANI	*In situ* polymerization	10	8	0.2	120	Sunlight	92	2.46	[115]
5	Ag-ZnO/PANI	*In situ* polymerization	200	8	0.2	120	Sunlight	98.6	2.61	[48]
6	TiO2/PVA	Hydrothermal method	15	-	10	50	600	95	-	[139]
		Mixing	2.5	-	11.5	360	56	70	-	[82]
7	ZnO/PVA	Sol-gel	10	7	16.7	90	400	70	3.11	[52]
		Mixing	20	7	8	80	400,000	95	-	[117]
8	Al2O3 - ZnO/PVA	Mixing	5	-		30	Sunlight	100	3. 21	[99]
9	TiO2/PDMS	Plasma treatment with UV illumination	1	-		120	Solar irradiation 680±150	23	3.42	[43]
		Mixing		-		30	48	75	-	[43]
10	CeO2 - TiO2/PANI	Galvanostatic	10	3		120	1200	96	2.26	[25]
11	Ag-TiO2/PAN	In-situ polymerization	5		2.0	55	Halogen lamp 500W	99.7,	2.24	[105]
12	SiO2 - TiO2/PANI	In-situ polymerization	10			90	100W	92	2.89	[129]
13	FeO-ZnO/PANI powder	In-situ polymerization	10			120	Sunlight	92, 1	3.01	[115]

Key: PVA-polyvinyl alcohol.
PDMS- Polydimethylsiloxane.

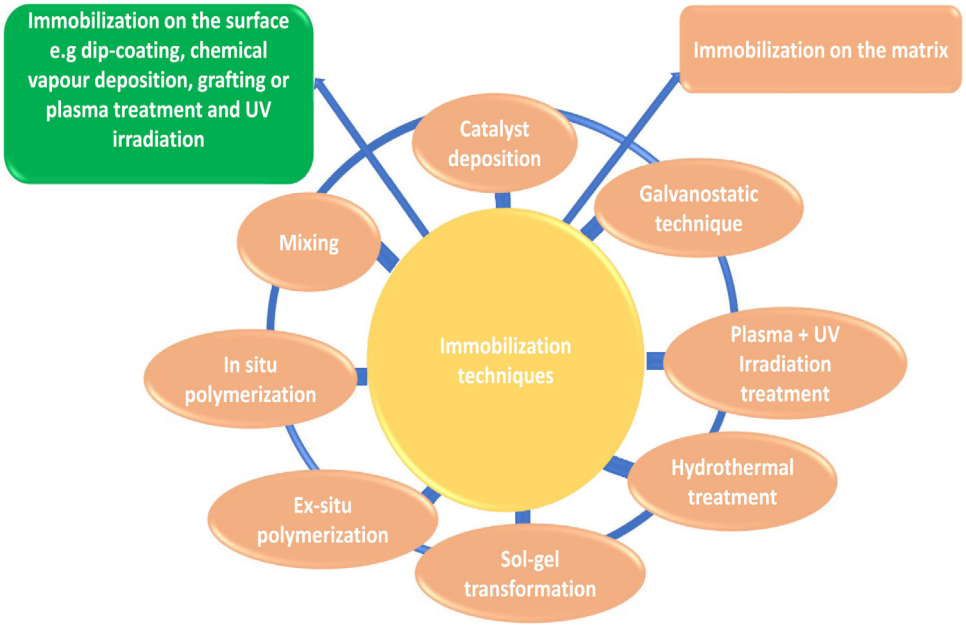

Fig. 10. Immobilization techniques for improved functional properties of nano-adsorbent.

Table 6
Nano polymeric composite of PANI as a catalyst in photocatalysis of some selected industrial dyes.

S/N	Nanocomposite catalyst	Degradation time (min)	Percentage degradation	Degraded Azo dyes	Source of light Rays	Ref.
1	PANI/Zr-Co	150	97%	Methylene Blue	UV	Aamir et al., 2015
2	Graphene/PANI	180	56%	Rose Bengal	Sunlight	[10]
3	PANI/Single walled Carbon nanotubes	10	98.6%	Rose Bengal	UV	Chatterjee et al., 2017
4	PANI/Single walled Carbon nanotubes	30	94.35%	methyl orange	UV	Chatterjee et al., 2017
5	PANI-hybrid defective Zn)	120	94%	methyl orange	UV	Pei et al., 2014
7	PANI-Modified TiO2 composite	125	81.3%	methyl orange	UV	[210]
8	PANI-Modified TiO2 composite	360	21.5%	methyl orange	Sunlight	[210]
9	TiO2/PPy/PANI	180	97%	victoria blue	Sunlight	[211]
10	TiO2/PPy/PANI	150	97%	Rose Bengal	Sunlight	[211]
11	2DhBN/PANI	90	93	methylene blue	UV	[112]
12	2DhBN/PANI	90	95	methyl orange	UV	[112]
14	TiO2/PANI	60	99.6%	methylene blue	UV	[157]
15	TiO2/PANI	30	96.5%	rhodamine b	UV	[157]
16	PANI/Nickel ferrate	150	97%	methylene blue		[158]
17	TiO2/PANI	45	92%	Acid blue 25	Sunlight	[107]
18	TiO2/PANI	45	95%	Acid Orange	Sunlight	[107]

of both positive and negative. This enhances the Pickering emulsions at the interface between organic solvents and aqueous solution leading to improved solubility of the polymer matrix [30]. Other techniques for the production of high profile multiple functionalized PANI based composites are photo-induced polymerization, interfacial polymerization, electrochemical polymerization, solution polymerization, seeding polymerization, emulsion polymerization, vapor phase self-assembling polymerization, plasma polymerization, and sonochemical synthesis process techniques [109]

Comparative evaluation of the photocatalytic performance of conventional catalyst and PANI composites

Table 6 shows the polyaniline nanocomposites with their respective degradation time and percentage, while Table 7 reveals the degradation time and percentage of conventional catalysts used in photocatalytic remediation of industrial azo dyes in wastewater. From Table 6, degradation percentage of 97% and 94.35% degradation of methylene blue at 150 min and 30 min respectively was recorded when the composite fabricated with PANI was used in the presence of UV radiation. Also, for methyl orange 94%,81.3%, and 95% degradation were obtained within 30, 125, and 90 min of photocatalysis. The observed time variation for the reaction is a function of the nature and composition of the composite and dyes, pH, dosage of the catalyst, contact time, and temperature (Reze et al., 2017). Furthermore, the composites of PANI used under influence of sunlight energy show a high percentage performance of 92%, 95% and 97% for the degradation of azo in Table 6 at

Table 7
Conventional nano composites in photocatalysis of some selected industrial dyes.

S/N	Catalyst	Degradation time (min)	Percentage degradation (%)	Degraded Azo dyes	Source of light Rays	Ref.
1	Fe-TiO2	120	46	Reactive violent 5	Sunlight	Antonio et al., 2019
2	TiO2	120	25	Reactive violent 5	Sunlight	Antonio et al., 2019
3	TiO2	40	25.90.5	Reactive orange 4	UV	[145]
4	TiO2	80	87.2	Reactive Black 5	UV	Zha and Guo, 2015
5	Cu/TiO2	180	21.8	Methyl Orange	Sunlight	[99]
6	TiO2 (nano tube array)	150	53	methyl orange	UV	Lakshmi and Rajagopalan, 2016
7	CU7S4 thin films with H2O2	180	81	Rose Bengal	Sunlight	Ghosh and Mondal, [143]
8	Poly(3-hexylthiophene)/TiO2	150	92.7	methyl orange	UV	Zhu and Dan, 2010
9	TiO2 nanoparticles using a triboelectric nanogenerator	120	76	methyl orange	UV	[145]
10	Au nanoparticles loaded graphitic carbon nitride nanosheets	150	92.6	methyl orange	Visible	
11	Cu(II) in presence of tartaric acid (for pH 3)	70	92	methyl orange	Visible	Guo et al. [144]
	TiO2	180	56	Acid blue 25	Sunlight	[107]
13	TiO2/G	120	97	methylene blue	UV	Gu et al., 2016
14	GO/TiO2	350	92	methylene blue	UV	Tseng et al., 2017
15	G/TiO2	180	90	methylene blue	UV	[10]
16	TiO2	45	73	Acid Orange 7	Sunlight	[107]

the rate of 45,45 and 180 min respectively. However, in Table 7 when sunlight irradiates the photocatalytic system using conventional catalyst low degradation percentage of 25%, 21.8%, and 56% for the industrial azo dyes at the longer duration of 120, 180 and 180 min was recorded. Ameen et al. [213] and Vargas et al. [191]) added that the faster photocatalytic reaction of PANI composite to sunlight energy was because of the conduction band of the semi-conductors used and the LUMO level of the PANI are well matched for the charge transfer. This consequently, promotes the electrons p–p* absorption band of the outside PANI film upon irradiation with sunlight light leading to faster reaction kinetics (Sadia et al., 2012; Rita et al., 2017). Also, when the same dyestuff present in the wastewater was comparatively assessed, at 90 min in Table 6, the degradation efficiency of methylene blue azo dye was 93% and 99.6% while in Table 7, 97%, 92%, and 90% were recorded at longer duration time of 120, 350, 180 min respectively for the same dye. Others include acid blue having percentage degradation of 95% and 73% at 45 min in Tables 6 and 7, respectively and Rose Bengal having 97% in 150 min in Table 2, while it has 81% in 180 min in Table 7. However, the low percentage of degradation of 56% from Table 2 of the same dye may be due to the adopted method of composite fabrication (Vargas et al. [191]).

Furthermore, the photosensitizing action of PANI when coupled with other semiconductors enhances the photocatalytic performance of the nanocomposites within a shorter duration as compared to its conventional counterpart (Muhd et al. [190]; Yang et al. [198]). This action is based on the narrow bandgap and enhanced charge mobility of PANI resulting in photon response as the energy level of PANI is incorporated into the semi-conductors [61,133]. Yang et al. [198] added that the synergistic effect between PANI and semiconductors such as TiO_2, makes it act as sensitizer for its large bandgap (3.2 eV), resulting in the reduction of the bandgap during photon excitation (Yang et al. [198]). The surface of the negatively charged TiO_2(rod) undergoes electrostatic interaction with positively charged anilium ion from the PANI forming a composite with improved the photocatalytic degradation of phenol in the azo at strong adsorption of light in the visible region (Yaseen and Scholz [214]). Furthermore, the use of PANI as a coating in in-situ polymerization of nanomaterial forestalls the possibility of recombination rate of electron-hole (e– – h+) by contributing to the bathochromic shift of the absorption band (Wang [207]; Yang et al. [198]; Jiang et al. [206]). Although, the use of metals as doping as a nanomaterial for the degradation of dyes comes with high dye degradation efficiency in Table 7 (92.6% and 92%). However, this technique is not cost-effective, not reproducible, and has a problem with catalyst recovery, hence it becomes imperative to use the alternative of nanocomposite developed from polyaniline (Yang et al. [199]; Abd El-Rady et al. [200]; Sood et al. [201]).

Table 8 shows various microorganism which serves as bio-catalysts used in the degradation of industrial azo dyes, their degradation time, and percentage. From the report in the Table, the microbial degradation of azo dye molecules from textile wastewater is characterized by a longer degradation time when compared to the photocatalyst used in Tables 6 and 7. The extended time makes the technique inappreciable for industrial commercialization owing to the slow dye decolorization rate and consequent generation of more toxic substances during continuous industrial dyeing and pigmentation processes. (Bruna et al. [178]) [55]. Also, from Table 8, only fungal laccase bio-catalyst has the lowest degradation time of 12 h to degrade 99% of methyl orange. This efficiency is based on its high redox potential (400 to 800 mV) resulting in the generation of intermediates via two distinct pathways [134]. However, one major setback of this bio-catalyst is that it is unstable at elevated temperatures and alkaline conditions, with which most effluent emerges after industrial usage (Shahzad and Burhan, [202]). This challenge, however, is an advantage to polymeric composites of polyaniline (Shahzad and Burhan, [202]). Other organisms from the Table exhibiting degradation at a duration lesser than 2 days are fungal *Aspergillus niger* having

Table 8
Conventional Bio-catalyst used in dye degradation.

S/N	Bio-catalyst	Degradation time	Percentage degradation	Degraded Azo dyes	Ref.
1	*Trametes versicolor, Ganoderma lucidum*	48h	90%	Reactive black 5	[146]
2	*Immobilized Trametes versicolor, Pleurotusostreatus and Phanerochaete chrysosporium Trametes versicolor*	4 days	90%	Reactive blue 4	[147]
3	*Trametes versicolor*	384h	90%	Reactive blue 4 Remazol	[159]
	Immobilized Trametespubescens and Pleurotusostreatus,	10 days	95%	Brilliant Blue R	[160]
4	*Trametes hirsute, Phanerochaete chrysosporium*	72hr	90%	Acid Blue	[161]
5	*Trametes hirsute, Marasmius sp.*	7 days	87%	Remazol Procion Blue H-EGN 125	[162]
			95%	Levafixblue E-RA	
			80%	Remazol Golden Yellow 3R l	
6	*Immobilized Phanerochaete chrysosporium*	120h	84%	Direct Violet 51,	[163]
			90%	Reactive Black 5 Ponceau	
			85%	Xylidine	
			86.7%	Bismark Brown	
7	*Aspergillus niger*	24h	98%	Acid Red 151,	[164]
			84%	Orange II	
8	*Aspergillus niger,*	36 h	99%	Congo red	[209]
9	*Ganoderma sp*	72 h	96.7%	Methyl Orange,	[165]
			75%	Crystal Violet	
			90%	Bromophenol Blue	
			91%	Malachite Green	
10	*Pseudomonas entomophila BS1*	120h	93%	Reactive black 5	[166]
11	*Laccase*		99%	digo carmine	[167]
			98%	Congo red	
			60%	Remazole Brilliant Blue R	
12	*Azoreductase*	120h	93%	Reactive black 5	[166]
13	*Laccase*	12h	99%	Methyl orange	[168]
14	Bacillus cereus	5 days	67%	Cibacron Black PSG, Cibacron Red P4B	[169]
15	*Bacillus subtilis*	5 days	97%	Reactive Red M8B	[170]
16	*Mutant Bacillus sp*. ACT2	37–48h	12–30%	Congo Red	[171]
17	*Pseudomonas sp*	24–35h	83%	Reactive Black 5	[212]
18	*Phanerochaete chrysosporium*	2 days	87%	Astrazon Red FBL	[172]

98%, 94% and 99% for Acid red 151, Orange II, and Congo red respectively, and *Pseudomonas sp* having 83% dye degradation at 24-33h for reactive black 5. It is also worthy of note to add that some of these microorganisms from the table have low degradation efficiency over an extended time. Examples of these are *Mutant Bacillus sp*. ACT2 with a degradation efficiency of 12–30% for Congo red at 37–48 h, *Bacillus cereus* having a degradation efficiency of 67% for Cibacron black PSG and Cibacron Red P4B during 5days. Although these bacteria cleave –N=N– bonds reductively and utilize amines as the source of carbon and energy for their growth. However, their stability to high pH, temperature, and the recalcitrant nature of some azo dyes remains a major challenge (Saratale et al. [203]; Mohammed and Burhan, 2014). Furthermore, the report by Buitrón et al [208] reveals that aerobic microbes cannot reduce azo linkages, their ability to destroy dye chromogens is lower when compared to the anaerobic bacterium. This justifies the low degradation of some bacterial microorganisms in Table 8. Other limiting tendencies of this bio-catalyst are problems of early saturation, making the nano-polymeric photocatalyst of greater industrial acceptance than the microorganism (Vikas et al., 2013; Shindhal et al. [150]).

Prospective challenges, key report findings and future out-look

The use of nano photoactive polymeric composites in photocatalysis incredibly proves to be most effective in performance during adsorption and degradation of toxic azo dyes appreciably present in the effluent. The study was able to establish the stability, flexibility, versatility cost-effectiveness, high performance and the possibility of recovery and reuse of the catalyst composite for treatment of pilot and field-scale wastewater. Additionally, the fabrication of this composite form polyaniline lowers the band gap and creates photon capturing possibility within the visible region, prevents agglomeration of Nps, lowers recombination of electron-hole pair and creates a more active site for binding of the dye molecules via tunability of the morphological properties of the NPs semiconductors used. Although the performance and the integrity of these nanomaterials are a function of the pathways of composite fabrication which is most efficient by the in-situ process. This process involves the incorporation of powered catalyst NPs into an immobilized conducting polymer matrix as stated by this review. However, factors such as irradiation intensity and source, contact time for adsorption-desorption equilibrium before photons are incident on the system, pH, temperature and initial dye concentration also play a vital role in the effective performance

of the process. The review also establishes the fact that among the varieties of semi-conductors used carbon-based nanomaterials stands due to their low toxicity, higher adsorption capacity and the excellent synergic effect when coupled with polyaniline to form composites. Hence, continued research should focus on the fabrication of nanocomposite using PANI coupled with carbon-based-nano materials, especially the multi-walled carbon nanotube (MWCNT), having unique morphological features fit for the adsorption and photodegradation process. Additionally, it is imperative to investigate more the possibility of recycling and recuse of the spent catalyst and to quantitatively determine the point of saturation of the fabricated composites during their reuses. It is worthy of note to add that the efficient primary treatment process must be given to textile effluent laden with dyes to remove the extraneous materials to limit the challenges of the photocatalytic process. Furthermore, the challenges of quantitative determination of initial dye concentration before photocatalysis limits the use of this treatment process due to oversaturation of the nano-catalyst at extremely high concentration dye molecules. Hence there is a need to create a robust industrial system to monitor the dye concertation fed into the photocatalytic reactor for effective use. Also, a future outlook on a hyphenated system of biological-photocatalytic techniques should be developed where biological microorganism such as laccase microbial enzymes associated with faster dye decolorizing speed is primarily used for the treatment of effluent before photocatalysis.

Declaration of Competing Interest

The authors declare an absence of competing financial interests in personal relationships that could influence the work reported in this paper

Acknowledgments

This work was supported and funded by Regional Scholarship for Innovation Fund (RSIF) a flagship program of the Partnership for Skills in Applied Sciences, Engineering and Technology (PASET).

References

[1] K. Abhishek, Conducting polymers: concepts and applications topical review, J. At. Mol. Condens. Nano Phys. 5 (2) (2018) 159–193 2018 ISSN 2349-2716 (online); 2349-6088 (print) Published by RGN Publications, doi:10.26713/jamcnp.v5i2.842.
[2] N. Abu, M. Fouzia, Application of Polyaniline-Based Adsorbents for Dye Removal from Water and Wastewater—a Review, Springer-Verlag GmbH Germany, Part of Springer Nature, 2018 23 September/Accepted: 12 December 2018.
[3] M.M. Adnan, A.R.M. Dalod, M.H. Balci, J. Glaum, M.A. Einarsrud, *In situ* synthesis of hybrid inorganic–polymer nanocomposites, Polymers 10 (10) (2018) 1129.
[4] L.A.A.R. Al-Rubaie, R.J. Mhessn, Synthesis and characterization of Azo dye para red and new derivatives, E J. Chem. 9 (1) (2012) 465–470, doi:10.1155/2012/206076.
[5] F. Alakhras, E. Alhajri, R. Haounati, H. Ouachtak, A.A. Addi, T.A. Saleh, A comparative study of photocatalytic degradation of Rhodamine B using natural-based zeolite composites, Surf. Interfaces 20 (May) (2020), doi:10.1016/j.surfin.2020.100611.
[6] A.M. Alansi, M. Al-Qunaibit, I.O. Alade, T.F. Qahtan, T.A. Saleh, Visible-light responsive BiOBr nanoparticles loaded on reduced graphene oxide for photocatalytic degradation of dye, J. Mol. Liq. 253 (2017) (2018) 297–304, doi:10.1016/j.molliq.2018.01.034.
[7] M.H. Alhaji, K. Sanaullah, A. Khan, A. Hamza, A. Muhammad, M.S. Ishola, A.R.H. Rigit, S.A. Bhawani, Recent developments in immobilizing titanium dioxide on supports for degradation of organic pollutants in wastewater-a review, Int. J. Environ. Sci. Technol. 14 (9) (2017) 2039–2052.
[8] T. Amakali, A. Živković, M.E.A. Warwick, D.R. Jones, C.W. Dunnill, L.S. Daniel, V. Uahengo, C.E. Mitchell, N.Y. Dzade, N.H. de Leeuw, Photocatalytic degradation of rhodamine b dye and hydrogen evolution by hydrothermally synthesized $NaBH_4$—spiked ZnS nanostructures, Front. Chem. 10 (April) (2022) 1–15, doi:10.3389/fchem.2022.835832.
[9] APHAStandard Methods for the Examination of Water and Waste Water, 22nd Ed., American Public Health Association, American Water Works Association, Water Environment Federation, 2012.
[10] S. Ameen, H.K. Seo, M. Shaheer Akhtar, H.S. Shin, Novel graphene/polyaniline nanocomposites and its photocatalytic activity toward the degradation of rose Bengal dye, Chem. Eng. J. 210 (2012) 220–228, doi:10.1016/j.cej.2012.08.035.
[11] E. Asgari, A. Esrafili, A.J. Jafari, R.R. Kalantary, H. Nourmoradi, M. Farzadkia, The comparison of ZnO/polyaniline nanocomposite under UV and visible radiations for decomposition of metronidazole: degradation rate, mechanism and mineralization, Process Saf. Environ. Prot. 128 (2019) 65–76.
[12] Y. Badr, M.G. Abd El-Wahed, M.A Mahmoud, Photocatalytic degradation of methyl red dye by silica nanoparticles, J. Hazard. Mater. 154 (1–3) (2008) 245–253, doi:10.1016/j.jhazmat.2007.10.020.
[13] A. Bafana, S.S. Devi, T. Chakrabarti, Azo dyes: past, present and the future, Environ. Rev. 19 (1) (2011) 350–370, doi:10.1139/a11-018.
[14] S. Balalaie, S. Ramezanpour, M. Bararjanian, J.H. Gross, DABCO-catalyzed efficient synthesis of naphthopyran derivatives via One-Pot three-component condensation reaction at room temperature, Synth. Commun. 38 (7) (2008) 1078–1089.
[15] P. Bansal, G.R. Chaudhary, S.K. Mehta, Comparative study of catalytic activity of ZrO_2 nanoparticles for sonocatalytic and photocatalytic degradation of cationic and anionic dyes, Chem. Eng. J. 280 (2015) 475–485, doi:10.1016/j.cej.2015.06.039.
[16] S. Benkhaya, S. M' rabet, A. El Harfi, A review on classifications, recent synthesis and applications of textile dyes, Inorg. Chem. Commun. 115 (2020) (March), doi:10.1016/j.inoche.2020.107891.
[17] M. Beygisangchin, S.A. Rashid, S. Shafie, A.R. Sadrolhosseini, Polyaniline thin films — a review, Polymers 13 (2021) 1–46.
[18] C.M. Bezerra de Araujo, G. Filipe Oliveira do Nascimento, G. Rodrigues Bezerra da Costa, K. Santos da Silva, A.M. Salgueiro Baptisttella, M. Gomes Ghislandi, M. Alves da Motta Sobrinho, Adsorptive removal of dye from real textile wastewater using graphene oxide produced via modifications of hummers method, Chem. Eng. Commun. 206 (11) (2019) 1375–1387.
[19] K.L. Bhowmik, K. Deb, A. Bera, R.K. Nath, B. Saha, Charge transport through polyaniline incorporated electrically conducting functional paper, J. Phys. Chem. C 120 (11) (2016) 5855–5860, doi:10.1021/acs.jpcc.5b08650.
[20] R. Borah, S. Banerjee, A. Kumar, Surface functionalization effects on structural, conformational, and optical properties of polyaniline nanofibers, Synth. Met. 197 (2014) 225–232.
[21] A. Bouarioua, M. Zerdaoui, Photocatalytic activities of TiO_2 layers immobilized on glass substrates by dip-coating technique toward the decolorization of methyl orange as a model organic pollutant, J. Environ. Chem. Eng. 5 (2) (2017) 1565–1574.
[22] S.B. Brachetti-Sibaja, D. Palma-Ramírez, A.M. Torres-Huerta, M.A. Domínguez-Crespo, H.J. Dorantes-Rosales, A.E. Rodríguez-Salazar, E. Ramírez-Meneses, Cvd conditions for mwcnts production and their effects on the optical and electrical properties of ppy/mwcnts, pani/mwcnts nanocomposites by *in situ* electropolymerization, Polymers 13 (3) (2021) 351.

[23] F. Can, X. Courtois, D. Duprez, Tungsten-based catalysts for environmental applications, Catalysts 11 (6) (2021) 703.
[24] Y.L. Chan, S.Y. Pung, S. Sreekantan, Synthesis of V_2O_5 nanoflakes on PET fiber as visible-light-driven photocatalysts for degradation of RhB dye, J. Catal. 2014 (2014) 1–7, doi:10.1155/2014/370696.
[25] C. Chen, D. Zhao, Q. Zhou, Y. Wu, X. Zhou, H. Wang, Facile preparation and characterization of polyaniline and CeO_2 co-decorated TiO_2 nanotube array and its highly efficient photoelectrocatalytic activity, Nanoscale Res. Lett. 14 (1) (2019) 1–9.
[26] M.N. Chong, B. Jin, C.W.K. Chow, C. Saint, Recent developments in photocatalytic water treatment technology: a review, Water Res. 44 (10) (2010) 2997–3027, doi:10.1016/j.watres.2010.02.039.
[27] K.T. Chung, Azo dyes and human health: a review, J. Environ. Sci. Health Part C Environ. Carcinog. Ecotoxicol. Rev. 34 (4) (2016) 233–261, doi:10.1080/10590501.2016.1236602.
[28] Dai, Wei-Lin, et al. "Tungsten containing materials as heterogeneous catalysts for green catalytic oxidation process." (2016): 1-27.
[29] N. Daneshvar, A. Oladegaragoze, N. Djafarzadeh, Decolorization of basic dye solutions by electrocoagulation: an investigation of the effect of operational parameters, J. Hazard. Mater. 129 (1–3) (2006) 116–122.
[30] A. Debnath, K. Deb, K. Sarkar, B. Saha, Low interfacial energy barrier and improved thermoelectric performance in Te-incorporated polypyrrole, J. Phys. Chem. C 125 (1) (2021) 168–177, doi:10.1021/acs.jpcc.0c09100.
[31] V.M. Dembitsky, T.A. Gloriozova, V.V. Poroikov, Pharmacological and predicted activities of natural azo compounds, Nat. Prod. Bioprospect. 7 (1) (2017) 151–169.
[32] C.S. Diko, Y. Qu, Z. Henglin, Z. Li, N. Ahmed Nahyoon, S. Fan, Biosynthesis and characterization of lead selenide semiconductor nanoparticles (PbSe NPs) and its antioxidant and photocatalytic activity, Arabian J. Chem. 13 (11) (2020) 8411–8423, doi:10.1016/j.arabjc.2020.06.005.
[33] L. Ding, B. Zou, W. Gao, Q. Liu, Z. Wang, Y. Guo, X. Wang, Y. Liu, Adsorption of Rhodamine-B from aqueous solution using treated rice husk-based activated carbon, Colloids Surf. A 446 (2014) 1–7.
[34] F.M. Drumond Chequer, G.A.R. de Oliveira, E.R. Anastacio Ferraz, J. Carvalho, M.V. Boldrin Zanoni, D.P de Oliveir, Textile dyes: dyeing process and environmental impact, in: Eco-Friendly Textile Dyeing and Finishing, INTECH, 2013, pp. 151–176.
[35] S. Dutta, B. Gupta, S.K. Srivastava, A.K. Gupta, Recent advances on the removal of dyes from wastewater using various adsorbents: a critical review, Mater. Adv. 2 (2021) 4497–4531.
[36] S. Dutta, B. Gupta, S.K. Srivastava, A.K. Gupta, Recent advances on the removal of dyes from wastewater using various adsorbents: a critical review, Mater. Adv. 2 (14) (2021) 4497–4531, doi:10.1039/d1ma00354b.
[37] G. Elango, S.M. Roopan, Efficacy of SnO_2 nanoparticles toward photocatalytic degradation of methylene blue dye, J. Photochem. Photobiol. B 155 (2016) 34–38, doi:10.1016/j.jphotobiol.2015.12.010.
[38] G. Fadillah, T.A. Saleh, H. Munawaroh, S. Wahyuningsih, A.H. Ramelan, Flow photocatalysis system-based functionalized graphene oxide-ZnO nanoflowers for degradation of a natural humic acid, Environ. Sci. Pollut. Res. 29 (7) (2022) 9883–9891, doi:10.1007/s11356-021-16333-9.
[39] G. Fadillah, T.A. Saleh, S. Wahyuningsih, Enhanced electrochemical degradation of 4-Nitrophenol molecules using novel Ti/TiO_2-NiO electrodes, J. Mol. Liq. 289 (2019), doi:10.1016/j.molliq.2019.111108.
[40] G. Ganapathy Selvam, K. Sivakumar, Phycosynthesis of silver nanoparticles and photocatalytic degradation of methyl orange dye using silver (Ag) nanoparticles synthesized from Hypnea musciformis (Wulfen) J.V. Lamouroux, Appl. Nanosci. (Switzerland) 5 (5) (2015) 617–622, doi:10.1007/s13204-014-0356-8.
[41] M. Ghaedi, Adsorption: Fundamental Processes and Applications, Academic Press, 2021.
[42] R. Giovannetti, E. Rommozzi, M. Zannotti, C.A D'Amato, Recent advances in graphene based TiO_2 nanocomposites ($GTiO_2Ns$) for photocatalytic degradation of synthetic dyes, Catalysts 7 (10) (2017), doi:10.3390/catal7100305.
[43] J. Gomes, B. Maniezo, P. Alves, P. Ferreira, R.C. Martins, Immobilization of TiO_2 onto a polymeric support for photocatalytic oxidation of a paraben's mixture, J. Water Process Eng. 46 (2022) 102458.
[44] I.J. Gómez, M. Vázquez Sulleiro, D. Mantione, N. Alegret, Carbon nanomaterials embedded in conductive polymers: a state of the art, Polymers 13 (5) (2021) 745.
[45] V.D. Gosavi, S. Sharma, Journal of environmental science, computer science and engineering & technology a general review on various treatment methods for textile wastewater, J. Environ. Sci. Comput. Sci. Eng. Technol. 3 (1) (2014) 29–39.
[46] Q. Guo, R. Ghadiri, T. Weigel, A. Aumann, E.L. Gurevich, C. Esen, O. Medenbach, W. Cheng, B. Chichkov, A. Ostendorf, Comparison of *in situ* and *ex situ* methods for synthesis of two-photon polymerization polymer nanocomposites, Polymers 6 (7) (2014) 2037–2050.
[47] A. Gürses, M. Açıkyıldız, K. Güneş, M.S. Gürses, Classification of dye and pigments, in: Dyes and Pigments, Springer, 2016, pp. 31–45.
[48] F. Habtamu, S. Berhanu, T. Mender, Polyaniline supported Ag-doped ZnO nanocomposite: synthesis, characterization, and kinetics study for photocatalytic degradation of malachite green, J. Chem. 2021 (2021) 2021.
[49] M. Heidarizad, S.S. Şengör, Synthesis of graphene oxide/magnesium oxide nanocomposites with high-rate adsorption of methylene blue, J. Mol. Liq. 224 (2016) 607–617.
[50] R. Hickman, E. Walker, S. Chowdhury, TiO_2-PDMS composite sponge for adsorption and solar mediated photodegradation of dye pollutants, J. Water Process Eng. 24 (2018) 74–82.
[51] C.N.C. Hitam, A.A. Jalil, A review on exploration of Fe_2O_3 photocatalyst towards degradation of dyes and organic contaminants, J. Environ. Manag. 258 (2020) 110050.
[52] S.S. Hossain, M. Tarek, T.D. Munusamy, K.M. Rezaul Karim, S.M. Roopan, S.M. Sarkar, C.K. Cheng, M.M. Rahman Khan, Facile synthesis of CuO/CdS heterostructure photocatalyst for the effective degradation of dye under visible light, Environ. Res. 188 (2020) 109803, doi:10.1016/j.envres.2020.109803.
[53] A. Huda, R. Ichwani, C.T. Handoko, M.D. Bustan, B. Yudono, F. Gulo, Comparative photocatalytic performances towards acid yellow 17 (AY17) and direct blue 71 (DB71) degradation using Sn_3O_4 flower-like structure, J. Phys. Conf. Ser. 1282 (1) (2019), doi:10.1088/1742-6596/1282/1/012097.
[54] N.K. Jangid, S. Jadoun, A. Yadav, M. Srivastava, N. Kaur, Polyaniline-TiO_2-based photocatalysts for dyes degradation, Polymer Bulletin, 78, 2021, doi:10.1007/s00289-020-03318-w.
[55] V. Jagadeesan, B. Sardhar, J. Josephraj, A review on efficacious methods to decolorize reactive azo dye 2013, J. Urban Environ. Eng. (JUEE) 7 (2013) 30–47 received 2 June 2012; received in revised form 28 March 2013; accepted 13 April 2013.
[56] M.A.C. Júnior, A.G. Santos, E.P. dos, Silva, G.F. Maimoni, H.N. Martins, M.L. Assis, M. de, C.A.C.M. Camargo, M.A.F. Camargo, Advances in the treatment of textile effluents: a review, OALib 06 (07) (2019) 1–13, doi:10.4236/oalib.1105549.
[57] V. Katheresan, Efficiency of Various Recent Wastewater Dye Removal Methods, J. Environ. Chem. Eng. 6 (2018) 4676–4697.
[58] I. Khan, K. Saeed, I. Khan, Nanoparticles: Properties, applications and toxicities, Arab. J. Chem. 12 (7) (2019) 908–931, doi:10.1016/j.arabjc.2017.05.011.
[59] M.I. Khan, M.K. Almesfer, A. Elkhaleefa, I. Shigidi, M.Z. Shamim, I.H. Ali, M. Rehan, Conductive polymers and their nanocomposites as adsorbents in environmental applications, Polymers (21) (2021) 13, doi:10.3390/polym13213810.
[60] T.W. Kim, Effect of pH and temperature for Photocatalytic degradation of organic compound on carbon-coated TiO_2, 3 (2) (2010) 193–198.
[61] Y.J. Lee, H.S. Lee, C.G. Lee, S.J. Park, J. Lee, S. Jung, G.A. Shin, Application of PANI/TiO_2 composite for photocatalytic degradation of contaminants from aqueous solution, Appl. Sci. 10 (19) (2020) 6710.
[62] C. Lei, M. Pi, D. Xu, C. Jiang, B. Cheng, Fabrication of hierarchical porous ZnO-Al_2O_3 microspheres with enhanced adsorption performance, Appl. Surf. Sci. 426 (2017) 360–368.
[63] T. Lei, J.Y. Wang, J. Pei, Design, synthesis, and structure–property relationships of isoindigo-based conjugated polymers, Acc. Chem. Res. 47 (4) (2014) 1117–1126.

[64] Z. Li, Y. Sun, J. Xing, Y. Xing, A. Meng, One step synthesis of Co/Cr-codoped ZnO nanoparticle with superb adsorption properties for various anionic organic pollutants and its regeneration, J. Hazard. Mater. 352 (2018) 204–214.
[65] G. Liao, Q. Li, Z. Xu, The chemical modification of polyaniline with enhanced properties: a review, Prog. Org. Coat. 126 (2019) 35–43.
[66] C.W. Lin, S. Xue, C. Ji, S.C. Huang, V. Tung, R.B. Kaner, Conducting polyaniline for antifouling ultrafiltration membranes: solutions and challenges, Nano Lett. 21 (9) (2021) 3699–3707, doi:10.1021/acs.nanolett.1c00968.
[67] O.F. Lopes, E.C. Paris, C. Ribeiro, Synthesis of Nb_2O_5 nanoparticles through the oxidant peroxide method applied to organic pollutant photodegradation: a mechanistic study, Appl. Catal. B 144 (2014) 800–808.
[68] L. Lou, R.J. Kendall, S. Ramkumar, Comparison of hydrophilic PVA/TiO_2 and hydrophobic PVDF/TiO_2 microfiber webs on the dye pollutant photo-catalyzation, J. Environ. Chem. Eng. 8 (5) (2020) 103914.
[69] F. Lu, D. Astruc, Nanocatalysts and other nanomaterials for water remediation from organic pollutants, Coord. Chem. Rev. 408 (2020) 213180.
[70] X. Lu, R. Liu, Treatment of azo dye-containing wastewater using integrated processes, Biodegradation of azo dyes (2010) 133–155.
[71] T. Lv, B. Li, Preparation of novel magnetic sodium alginate-ferric (III) gel beads and their super-efficient removal of direct dyes from water, J. Polym. Environ. 29 (5) (2021) 1576–1590.
[72] K. MA, A. M, Membrane applications of polyaniline based nano-composite ion-exchanger and its electrochemical properties for desalination, J. Membr. Sci. Technol. 6 (2) (2016), doi:10.4172/2155-9589.1000152.
[73] A. Mahapatra, B.G. Mishra, G. Hota, Adsorptive removal of congo red dye from wastewater by mixed iron oxide–alumina nanocomposites, Ceram. Int. 39 (5) (2013) 5443–5451.
[74] M. Maruthapandi, L. Eswaran, J.H.T. Luong, A. Gedanken, Sonochemical preparation of polyaniline@TiO_2 and polyaniline@SiO_2 for the removal of anionic and cationic dyes, Ultrason. Sonochem. 62 (2020) 104864 March 2021, doi:10.1016/j.ultsonch.2019.104864.
[75] A.K. Mishra, Conducting polymers: concepts and applications, J. At. Mol. Condens. Nano Phys. 5 (2) (2018) 159–193, doi:10.26713/jamcnp.v5i2.842.
[76] S. Saha, N. Chaudhary, A. Kumar, M. Khanuja, Polymeric nanostructures for photocatalytic dye degradation: polyaniline for photocatalysis, SN Applied Sciences 2 (6) (2020) 1–10.
[77] M. Mitra, K. Kargupta, S. Ganguly, S. Goswami, D. Banerjee, Facile synthesis and thermoelectric properties of aluminum doped zinc oxide/polyaniline (AZO/PANI) hybrid, Synth. Met. 228 (2017) 25–31 October, doi:10.1016/j.synthmet.2017.03.017.
[78] S. Mkata, Uv vis spectroscopy practical, Phys. Chem. Prakt. I (2017) 1–11 https://www.coursehero.com/file/76918963/UVVis-HS17pdf/.
[79] R.M. Mohamed, A. Shawky, I.A. Mkhalid, Facile synthesis of MgO and Ni-MgO nanostructures with enhanced adsorption of methyl blue dye, J. Phys. Chem. Solids 101 (2017) 50–57.
[80] A.M. Mohammed, S.S. Mohtar, F. Aziz, M. Aziz, A. Ul-Hamid, Cu_2O/ZnO-PANI ternary nanocomposite as an efficient photocatalyst for the photodegradation of Congo Red dye, J. Environ. Chem. Eng. 9 (2) (2021) 105065.
[81] K. Mondal, A. Sharma, in: Photocatalytic Oxidation of Pollutant Dyes in Wastewater by TiO_2 and ZnO nano-materials – A Mini-review, Indian Institute of Tecnology, 2016, pp. 36–72. January 2015.
[82] A.D.S. Montallana, B.Z. Lai, J.P. Chu, M.R. Vasquez, Enhancement of photodegradation efficiency of PVA/TiO_2 nanofiber composites via plasma treatment, Mater. Today Commun. 24 (2020) 101183.
[83] O. Moradi, G. Sharma, Emerging novel polymeric adsorbents for removing dyes from wastewater: a comprehensive review and comparison with other adsorbents, Environ. Res. 201 (June) (2021) 111534, doi:10.1016/j.envres.2021.111534.
[84] B. Mu, J. Tang, L. Zhang, A. Wang, Facile fabrication of superparamagnetic graphene/polyaniline/Fe_3O_4 nanocomposites for fast magnetic separation and efficient removal of dye, Sci. Rep. 7 (1) (2017) 1–12.
[85] N. Muhd Julkapli, S. Bagheri, S. Bee Abd Hamid, Recent advances in heterogeneous photocatalytic decolorization of synthetic dyes, Sci. World J. (2014) 2014, doi:10.1155/2014/692307.
[86] K. Nirmala, et al., Polyaniline TiO_2 based photocatalysts for dyes degradation, Polym. Bull. (2020) Received: 20 March 2020 /Revised: 12 June 2020 / Accepted: 26 July 2020 © Springer-Verlag GmbH Germany, part of Springer Nature 2020, doi:10.1007/s00289-020-03318-w.
[87] A. Nasar, F. Mashkoor, Application of polyaniline-based adsorbents for dye removal from water and wastewater—a review, Environ. Sci. Pollut. Res. 26 (6) (2019) 5333–5356, doi:10.1007/s11356-018-3990-y.
[88] B.A. Oni, S.E. Sanni, Cationic graphene-based polymer composite modified with chromium-based metal-organic framework [GP/MIL-53 (Cr)] for the degradation of 2, 4-dichlorophenol in aqueous solution, Mater. Today Sustain. 18 (2022) 100134.
[89] S. Phoemphoonthanyakit, P. Seeharaj, P. Damrongsak, K. Locharoenrat, Effect of adsorption characteristics of rhodamine 6G dye solution in Fe_3O_4 magnetic nanoparticles on fluorescence quantum yield, J. Spectrosc. 2019 (2019).
[90] A.V. Popoola, The Chemistry of Colours in Dyes and Pigments, Witd Publishing Ltd, 2015.
[91] N. Qutub, P. Singh, S. Sabir, S. Sagadevan, W.C. Oh, Enhanced photocatalytic degradation of acid blue dye using CdS/TiO_2 nanocomposite, Sci. Rep. 12 (1) (2022) 1–19, doi:10.1038/s41598-022-09479-0.
[92] A. Ragunathan, R. Krishnan, B. Ameen Kamaludeen, Stability of tungsten oxide nanoparticles in different media, J. Chem. Res. 39 (11) (2015) 622–626, doi:10.3184/174751915x14446446579178.
[93] G. Rajesh, S. Akilandeswari, D. Govindarajan, K. Thirumalai, Enhancement of photocatalytic activity of ZrO_2 nanoparticles by doping with Mg for UV light photocatalytic degradation of methyl violet and methyl blue dyes, J. Mater. Sci. Mater. Electron. 31 (5) (2020) 4058–4072, doi:10.1007/s10854-020-02953-3.
[94] M. Ramesh, CuO as efficient photo catalyst for photocatalytic decoloration of wastewater containing Azo dyes, Water Pract. Technol. 16 (4) (2021) 1078–1090, doi:10.2166/wpt.2021.067.
[95] M. Ramesh, M.P.C. Rao, S. Anandan, H. Nagaraja, Adsorption and photocatalytic properties of NiO nanoparticles synthesized via a thermal decomposition process, J. Mater. Res. 33 (5) (2018) 601–610, doi:10.1557/jmr.2018.30.
[96] E. Rayappan, J. Muthaian, M. Pandi, Investigation on the photocatalytic activity of chemically synthesized zirconium doped cadmium selenide nanoparticles for indigo carmine dye degradation under solar light irradiation, J. Water Environ. Nanotechnol. 6 (2) (2021) 177–187, doi:10.22090/jwent.2021.02.07.
[97] K.R. Reddy, M.S. Jyothi, A.V Raghu, V. Sadhu, S. Naveen, T.M. Aminabhavi, Nanocarbons-supported and polymers-supported titanium dioxide nanostructures as efficient photocatalysts for remediation of contaminated wastewater and hydrogen production, in: Nanophotocatalysis and Environmental Applications, Springer, 2020, pp. 139–169.
[98] M. Ren, F.H. Frimmel, G. Abbt-Braun, Multi-cycle photocatalytic degradation of bezafibrate by a cast polyvinyl alcohol/titanium dioxide (PVA/TiO_2) hybrid film, J. Mol. Catal. A Chem. 400 (2015) 42–48.
[99] N. Riaz, F.K. Chong, Z.B. Man, B.K. Dutta, R.M. Ramli, M.S. Khan, Visible light photodegradation of azo dye by Cu/TiO_2, Adv. Mater. Res. 917 (June) (2014) 151–159, doi:10.4028/www.scientific.net/AMR.917.151.
[100] R.D. Saini, Textile organic dyes : polluting effects and elimination methods from textile waste water, Int. J. Chem. Eng. Res. 9 (1) (2017) 121–136.
[101] S. Saha, N. Chaudhary, A. Kumar, M. Khanuja, Polymeric nanostructures for photocatalytic dye degradation: polyaniline for photocatalysis, SN Appl. Sci. 2 (6) (2020) 1–10, doi:10.1007/s42452-020-2928-4.
[102] B. Said, R. Souad M', E.H. Ahmed, A review on classifications, recent synthesis and applications of textile dyes, Inorg. Chem. Commun. (2020) 107891 March.
[103] T.A. Saleh, V.K. Gupta, Photo-catalyzed degradation of hazardous dye methyl orange by use of a composite catalyst consisting of multi-walled carbon nanotubes and titanium dioxide, J. Colloid Interface Sci. 371 (1) (2012) 101–106, doi:10.1016/j.jcis.2011.12.038.
[104] M.A.M. Salleh, D.K. Mahmoud, W.A.W.A. Karim, A. Idris, Cationic and anionic dye adsorption by agricultural solid wastes: a comprehensive review, Desalination 280 (1–3) (2011) 1–13.

[105] S. Sambaza, A. Maity, K. Pillay, Enhanced degradation of BPA in water by PANI supported Ag/TiO_2 nanocomposite under UV and visible light, J. Environ. Chem. Eng. 7 (1) (2019) 102880.
[106] S. Samsami, M. Mohamadi, M.H. Sarrafzadeh, E.R. Rene, M. Firoozbahr, Recent advances in the treatment of dye-containing wastewater from textile industries: overview and perspectives, Process Saf. Environ. Prot. 143 (2020) 138–163 May, doi:10.1016/j.psep.2020.05.034.
[107] Sandhya, K.P., Haridas, S., & Sugunan, S. (2013). Visible light induced photocatalytic activity of polyaniline modified TiO2 and Clay-TiO2 composites. 8(2), 145–153. 10.9767/bcrec.8.2.4949.145-153
[108] R. Saravanan, E. Sacari, F. Gracia, M.M. Khan, E. Mosquera, V.K. Gupta, Conducting PANI stimulated ZnO system for visible light photocatalytic degradation of coloured dyes, J. Mol. Liq. 221 (2016) 1029–1033.
[109] K. Sarkar, K. Deb, A. Debnath, A. Bera, A. Debnath, B. Saha, Polaron localization in polyaniline through methylene blue dye interaction for tuned charge transport and optical properties, Colloid. Polym. Sci. 296 (12) (2018) 1927–1934, doi:10.1007/s00396-018-4419-3.
[110] K. Sarkar, A. Debnath, K. Deb, A. Bera, B. Saha, Effect of NiO incorporation in charge transport of polyaniline: improved polymer based thermoelectric generator, Energy 177 (2019) 203–210, doi:10.1016/j.energy.2019.04.045.
[111] S. Sarkar, A. Banerjee, U. Halder, R. Biswas, R. Bandopadhyay, Degradation of synthetic azo dyes of textile industry: a sustainable approach using microbial enzymes, Water Conserv. Sci. Eng. 2 (4) (2017) 121–131, doi:10.1007/s41101-017-0031-5.
[112] S. Shahabuddin, R. Khanam, M. Khalid, N.M. Sarih, J.J. Ching, S. Mohamad, R. Saidur, Synthesis of 2D boron nitride doped polyaniline hybrid nanocomposites for photocatalytic degradation of carcinogenic dyes from aqueous solution, Arab. J. Chem. 11 (6) (2018) 1000–1016, doi:10.1016/j.arabjc.2018.05.004.
[113] N.S.M. Shahrodin, J. Jaafar, A.R. Rahmat, N. Yusof, M.H. Dzarfan Othman, M.A. Rahman, Superparamagnetic iron oxide as photocatalyst and adsorbent in wastewater treatment–a review, Micro Nanosyst. 12 (1) (2020) 4–22.
[114] G.S. Shankarling, P.P. Deshmukh, A.R. Joglekar, Process intensification in azo dyes, J. Environ. Chem. Eng. 5 (4) (2017) 3302–3308.
[115] S. Sharma, G. Sharma, A. Kumar, M. Naushad, G.T. Mola, A. Kumar, F.A. Al-Misned, H.A. El-Serehy, F.J. Stadler, Visibly active FeO/ZnO@ PANI magnetic nano-photocatalyst for the degradation of 3-aminophenol, Top. Catal. 63 (11) (2020) 1302–1313.
[116] W.S. Shin, Competitive sorption of anionic and cationic dyes onto cetylpyridinium-modified montmorillonite, J. Environ. Sci. Health Part A 43 (12) (2008) 1459–1470.
[117] M.J. Silva, J. Gomes, P. Ferreira, R.C. Martins, An overview of polymer-supported catalysts for wastewater treatment through light-driven processes, Water (Switzerland) 14 (5) (2022) 1–34, doi:10.3390/w14050825.
[118] N.B. Singh, A. Agarwal, K. Rachna, Adsorptive and photocatalytic removal of rhodamine B Dye from water by using copper ferrite polyaniline nanocomposite, J. Sci. Ind. Res. (JSIR) 79 (06) (2020) 558–561.
[119] N. Singh, J. Prakash, M. Misra, A. Sharma, R.K. Gupta, Dual functional Ta-doped electrospun TiO_2 nanofibers with enhanced photocatalysis and SERS detection for organic compounds, ACS Appl. Mater. Interfaces 9 (34) (2017) 28495–28507.
[120] S. Singh, H. Mahalingam, P.K. Singh, Polymer-supported titanium dioxide photocatalysts for environmental remediation: A review, Appl. Catal. A 462 (2013) 178–195.
[121] M. Sivakumar, S. Yadav, W.S. Hung, J.Y. Lai, One-pot eco-friendly synthesis of edge-carboxylate graphene via dry ball milling for enhanced removal of acid and basic dyes from single or mixed aqueous solution, J. Clean. Prod. 263 (2020) 121498.
[122] J. Smita, J. Dipika, K. Shraddha, Polyaniline for removal of methyl orange dye from wastewater, Int. J. Sci. Eng. Manag. (IJSEM) 1 (1) (2016) 1–6 https://www.technoarete.org/common_abstract/pdf/IJSEM/v1/i1/1.pdf.
[123] K. Suttiponparnit, J. Jiang, M. Sahu, S. Suvachittanont, T. Charinpanitkul, P. Biswas, Role of surface area, primary particle size, and crystal phase on titanium dioxide nanoparticle dispersion properties, Nanoscale Res. Lett. 6 (1) (2011) 1–8, doi:10.1007/s11671-010-9772-1.
[124] M.B. Tahir, M. Sohaib, M. Sagir, M. Rafique, Role of nanotechnology in photocatalysis, in: Encyclopedia of Smart Materials, PubMed, 2022, pp. 578–589. January.
[125] W.Y. Teoh, J.A. Scott, R. Amal, Progress in heterogeneous photocatalysis: from classical radical chemistry to engineering nanomaterials and solar reactors, J. Phys. Chem. Lett. 3 (5) (2012) 629–639.
[126] B.M. Thamer, A. Aldalbahi, A. Moydeen, MH Effective adsorption of Coomassie brilliant blue dye using poly (phenylene diamine) grafted electrospun carbon nanofibers as a novel adsorbent, Mater. Chem. Phys 234 (2019) 133–145.
[127] B.D.C. Ventura-camargo, M.A. Marin-morales, Azo dyes: characterization and toxicity– a review, Text. Light Ind. Sci. and Technol. (TLIST) (2013) May 2013.
[128] B.D.C. Ventura-camargo, M.A. Marin-morales, Azo dyes: characterization and toxicity– a review, Text. Light Ind. Sci. and Technol. (TLIST) 2 (2) (2013) 85–103.
[129] S. Wahyuni, E.S. Kunarti, R.T. Swasono, I. Kartini, Characterization and photocatalytic activity of TiO_2(rod)-SiO_2-polyaniline nanocomposite, Indones. J. Chem. 18 (2) (2018) 321–330, doi:10.22146/ijc.22550.
[130] N. Wang, G. Yang, H. Wang, R. Sun, C.P. Wong, Visible light-responsive photocatalytic activity of boron nitride incorporated composites, Front. Chem. 6 (2018) 1–12 September, doi:10.3389/fchem.2018.00440.
[131] M. Waseem, S. Munsif, U. Rashid, Imad-ud-Din, Physical properties of α-Fe_2O_3 nanoparticles fabricated by modified hydrolysis technique, Appl. Nanosc. (Switzerland) 4 (5) (2014) 643–648, doi:10.1007/s13204-013-0240-y.
[132] J.K.H. Wong, H.K. Tan, S.Y. Lau, P.S. Yap, M.K. Danquah, Potential and challenges of enzyme incorporated nanotechnology in dye wastewater treatment: a review, J. Environ. Chem. Eng. 7 (4) (2019) 103261.
[133] C. Yang, W. Dong, G. Cui, Y. Zhao, X. Shi, X. Xia, B. Tang, W. Wang, Enhanced photocatalytic activity of PANI/TiO_2 due to their photosensitization-synergetic effect, Electrochim. Acta 247 (2017) 486–495.
[134] J. Yang, X. Yang, Y. Lin, T.B. Ng, J. Lin, X. Ye, Laccase-catalyzed decolorization of malachite green: performance optimization and degradation mechanism, PLoS One 10 (5) (2015) e0127714.
[135] H.S. Zakria, M.H.D. Othman, R. Kamaludin, S.H.S.A. Kadir, T.A. Kurniawan, A. Jilani, Immobilization techniques of a photocatalyst into and onto a polymer membrane for photocatalytic activity, RSC Adv. 11 (12) (2021) 6985–7014.
[136] E.N. Zare, A. Motahari, M. Sillanpää, Nanoadsorbents based on conducting polymer nanocomposites with main focus on polyaniline and its derivatives for removal of heavy metal ions/dyes: a review, Environ. Res. 162 (2018) 173–195 January, doi:10.1016/j.envres.2017.12.025.
[137] K. Zhang, M. Davis, J. Qiu, L. Hope-Weeks, S. Wang, Thermoelectric properties of porous multi-walled carbon nanotube/polyaniline core/shell nanocomposites, Nanotechnology 23 (38) (2012) 385701.
[138] Q. Zhang, S. Wang, H. Fu, Y. Wang, K. Yu, L. Wang, Facile design and hydrothermal synthesis of In_2O_3 nanocube polycrystals with superior triethylamine sensing properties, ACS Omega 5 (20) (2020) 11466–11472, doi:10.1021/acsomega.0c00497.
[139] H. Zhao, Z. Li, X. Lu, W. Chen, Y. Cui, B. Tang, J. Wang, X. Wang, Fabrication of PANI@ TiO_2 nanocomposite and its sunlight-driven photocatalytic effect on cotton fabrics, J. Text. Inst. 112 (11) (2021) 1850–1858.
[140] Y. Zheng, B. Cheng, W. You, J. Yu, W. Ho, 3D hierarchical graphene oxide-NiFe LDH composite with enhanced adsorption affinity to Congo red, methyl orange and Cr (VI) ions, J. Hazard. Mater. 369 (2019) 214–225.
[141] P. Zhou, J. Li, W. Yang, L. Zhu, H. Tang, Polyaniline nanofibers: their amphiphilicity and uses for pickering emulsions and on-demand emulsion separation, Langmuir 34 (8) (2018) 2841–2848.
[142] A. Zuorro, R. Lavecchia, M.M. Monaco, G. Iervolino, V. Vaiano, Photocatalytic degradation of azo dye reactive, Catalysts 9 (2019) 645–661.
[143] A. Ghosh, A. Mondal, A simple electrochemical route to deposit Cu_7S_4 thin films and their photocatalytic properties, Appl. Surf. Sci. 328 (2015) 63–70.
[144] X.C Guo, Y. Shi, Y. Lan, C. Qin, Rapid photodegradation of methyl orange (MO) assisted with Cu(II) and tartaric acid, PLoS One 10 (8) (2015) e0134298.
[145] Y. Su, Y. Yang, H. Zhang, Y. Xie, Z. Wu, Y. Jiang, N. Fukata, Y. Bando, Z.L. Wang, Enhanced photodegradation of methyl orange with TiO_2 nanoparticles using a triboelectric nanogenerator, Nanotechnology 24 (2013) 295401.

[146] R. Baccar, P. Blanquez, J. Bouzid, M. Feki, H. Attiya, M. Sarra, Decolorization of a tannery dye: from fungal screening to bioreactor application, Biochemical engineering journal 56 (3) (2011) 184–189.
[147] S. Pilatin, B. Kunduhoğlu, Decolorization of textile dyes by newly isolated Trametes versicolor strain, Anadolu University Journal of Science and Technology C-Life Sciences and Biotechnology 1 (2) (2011) 125–136.
[148] K. V. Vimalnath, A. Rajeswari, K. C. Jagadeesan, C. Viju, P. V. Joshi, M. Venkatesh, Studies on the production feasibility of 64Cu by (n, p) reactions on Zn targets in Dhruva research reactor, Journal of Radioanalytical and Nuclear Chemistry 294 (1) (2012) 43–47.
[149] M. R. Rekha, C. P. Sharma, Synthesis and evaluation of lauryl succinyl chitosan particles towards oral insulin delivery and absorption, Journal of Controlled Release 135 (2) (2009) 144–151.
[150] T. Shindhal, P. Rakholiya, S. Varjani, A. Pandey, H. H. Ngo, W. Guo, M. J. Taherzadeh, A critical review on advances in the practices and perspectives for the treatment of dye industry wastewater, Bioengineered 12 (1) (2021) 70–87.
[151] C. Zaharia, R. Diaconescu, M. Surpăţeanu, Study of flocculation with Ponilit GT-2 anionic polyelectrolyte applied into a chemical wastewater treatment, Open Chemistry 5 (1) (2007) 239–256.
[152] Z. Carmen, S. Daniela, in: Textile organic dyes-characteristics, polluting effects and separation/elimination procedures from industrial effluents-a critical overview, (Vol. 3„ IntechOpen, Rijeka, 2012, pp. 55–86.
[153] S. Ibeid, M. Elektorowicz, J. A. Oleszkiewicz, Novel electrokinetic approach reduces membrane fouling, Water research 47 (16) (2013) 6358–6366.
[154] R. Rosal, A. Rodríguez, J. A. Perdigón-Melón, A. Petre, E. García-Calvo, M. J. Gómez, A. R. Fernández-Alba, Degradation of caffeine and identification of the transformation products generated by ozonation, Chemosphere 74 (6) (2009) 825–831.
[155] E. S. P. Prado, F. S. Miranda, de Araujo, G. L. Fernandes, A. J. Pereira, M. C. Gomes, G. Petraconi, Physicochemical Modifications and Decolorization of Textile Wastewater by Ozonation: Performance Evaluation of a Batch System, Ozone: Science & Engineering (2022) 1–15.
[156] A. K. Pandey, R. R. Kumar, B. Kalidasan, I. A. Laghari, M. Samykano, R. Kothari, V. V. Tyagi, Utilization of solar energy for wastewater treatment: Challenges and progressive research trends, Journal of Environmental Management 297 (2021) 113300.
[157] Y. Tao, S. Li, S. Zhao, D. Li, Y. Wu, Z. Liang, H. Cheng, TiO2/PANI/Graphene–PVA hydrogel for recyclable and highly efficient photo-electrocatalysts, Industrial & Engineering Chemistry Research 60 (28) (2021) 10033–10043.
[158] M. R. Patil, V. S. Shrivastava, Photocatalytic degradation of carcinogenic methylene blue dye by using polyaniline-nickel ferrite nano-composite, Der Chemica Sinica 5 (2) (2014) 8–17.
[159] H. Yemendzhiev, Z. Alexieva, A. Krastanov, Decolorization of synthetic dye reactive blue 4 by mycelial culture of white-rot fungi Trametes versicolor 1, Biotechnology & Biotechnological Equipment 23 (3) (2009) 1337–1339.
[160] M. Aghaie-Khouzani, H. Forootanfar, M. Moshfegh, M. R. Khoshayand, M. A. Faramarzi, Decolorization of some synthetic dyes using optimized culture broth of laccase producing ascomycete Paraconiothyrium variabile, Biochemical Engineering Journal 60 (2012) 9–15.
[161] R. Tapia-Tussell, D. Pérez-Brito, R. Rojas-Herrera, A. Cortes-Velazquez, G. Rivera-Muñoz, S. Solis-Pereira, New laccase-producing fungi isolates with biotechnological potential in dye decolorization, African Journal of Biotechnology 10 (50) (2011) 10134–10142.
[162] J. P. Jadhav, D. C. Kalyani, A. A. Telke, S. S. Phugare, S. P. Govindwar, Evaluation of the efficacy of a bacterial consortium for the removal of color, reduction of heavy metals, and toxicity from textile dye effluent, Bioresource Technology 101 (1) (2010) 165–173.
[163] E. Lamizadeh, N. Enayatizamir, H. Motamedi, Isolation and identification of plant growth-promoting rhizobacteria (PGPR) from the rhizosphere of sugarcane in saline and non-saline soil, International Journal of Current Microbiology and Applied Sciences 5 (10) (2016) 1072–1083.
[164] N. Ali, A. Hameed, M. Siddiqui, P. B. Ghumro, S. Ahmed, Application of Aspergillus niger SA1 for the enhanced bioremoval of azo dyes in simulated textile effluent, African Journal of Biotechnology 8 (16) (2009).
[165] R. Zhuo, L. Ma, F. Fan, Y. Gong, X. Wan, M. Jiang, Y. Yang, Decolorization of different dyes by a newly isolated white-rot fungi strain Ganoderma sp. En3 and cloning and functional analysis of its laccase gene, Journal of hazardous materials 192 (2) (2011) 855–873.
[166] S. Khan, A. Malik, Degradation of Reactive Black 5 dye by a newly isolated bacterium Pseudomonas entomophila BS1, Canadian journal of microbiology 62 (3) (2016) 220–232.
[167] R. Mehta, P. Singhal, H. Singh, D. Damle, A. K. Sharma, Insight into thermophiles and their wide-spectrum applications. 3, Biotech 6 (1) (2016) 1–9.
[168] L. N. Du, G. Li, Y. H. Zhao, H. K. Xu, Y. Wang, Y. Zhou, L. Wang, Efficient metabolism of the azo dye methyl orange by Aeromonas sp. strain DH-6: characteristics and partial mechanism, International Biodeterioration & Biodegradation 105 (2015) 66–72.
[169] I. O. Ola, A. K. Akintokun, I. Akpan, I. O. Omomowo, V. O. Areo, Aerobic decolourization of two reactive azo dyes under varying carbon and nitrogen source by Bacillus cereus, African Journal of Biotechnology 9 (5) (2010).
[170] P. Arulazhagan, A study on microbial decolourization of reactive red M8B by Bacillus subtilis isolated from dye contaminated soil samples, Int J Curr Res Biol Med 1 (1) (2016) 1–13.
[171] K. P. Gopinath, S. Murugesan, J. Abraham, K. Muthukumar, Bacillus sp. mutant for improved biodegradation of Congo red: random mutagenesis approach, Bioresource technology 100 (24) (2009) 6295–6300.
[172] M. Sedighi, A. Karimi, F. Vahabzadeh, Involvement of ligninolytic enzymes of Phanerochaete chrysosporium in treating the textile effluent containing Astrazon Red FBL in a packed-bed bioreactor, Journal of Hazardous Materials 169 (1–3) (2009) 88–93.
[173] J. O. Oyetade, A. Oluwafemi, A. Olumide, Tensile Properties and Dye Uptake Assessment of Cotton Fabrics Sized with Corn (Zea mays) Starch and Sorghum (Sorghum bicolor) Starch, Earthline Journal of Chemical Sciences 5 (1) (2021) 49–62.
[174] A.O. Adetuyi, J. Jabar, J.A . Oyetade, U. Judith, A. Taiwo, F. Moyo, Preparation and performance evaluation of an active anti-bleeding solution for laundering multicoloured textile apparels, Chemistry Journal 5 (1) (2020) 1–14.
[175] J. A. Oyetade, A. Adetuyi, J. Jabar, U. Judith, A. Taiwo, F. Moyo, Tensile Strength Assessment and Effluent Analysis of Multicoloured Textile Apparels Laundered in Anti-bleeding Solution, International Journal of Advanced Materials Research 6 (4) (2020) 54–60.
[176] M. A. Rauf, S. S. Ashraf, Fundamental principles and application of heterogeneous photocatalytic degradation of dyes in solution, Chemical engineering journal 151 (1–3) (2009) 10–18.
[177] M. Sudha, A. Saranya, G. Selvakumar, N. Sivakumar, Microbial degradation of azo dyes: a review, International Journal of Current Microbiology and Applied Sciences 3 (2) (2014) 670–690.
[178] Bruna, C.V., Maria A M (2013). “Azo Dyes: Characterization and Toxicity–A.” Textiles and Light Industrial Science and Technology (TLIST) Volume 2 Issue 2, April 2013
[179] M Vinothkannan, C Karthikeyan, G Gnana Kumar, One-pot green synthesis of reduced graphene oxide (RGO)/ Fe3O4nanocomposites and its catalytic activity toward methylene blue dye degradation, Spectrochim Acta A Mol Biomol Spectrosc 136 (2015) 256–264, doi:10.1016/j.saa.2014.09.031.
[180] B. D. C. Ventura-Camargo, P. P. Maltempi, M. A. Marin-Morales, The use of the cytogenetic to identify mechanisms of action of an azo dye in Allium cepa meristematic cells, J Environ Anal Toxicol 1 (3) (2011) 1–12.
[181] N. K. Jangid, S. Jadoun, N. Kaur, A review on high-throughput synthesis, deposition of thin films and properties of polyaniline, European Polymer Journal 125 (2020) 109485.
[182] R. Comparelli, E. Fanizza, M. L. Curri, P. D. Cozzoli, G. Mascolo, A. Agostiano, UV-induced photocatalytic degradation of azo dyes by organic-capped ZnO nanocrystals immobilized onto substrates, Applied Catalysis B: Environmental 60 (1–2) (2005) 1–11.
[183] X. D. Zhu, Y. J. Wang, R. J. Sun, D. M. Zhou, Photocatalytic degradation of tetracycline in aqueous solution by nanosized TiO2, Chemosphere 92 (8) (2013) 925–932.
[184] T. Soltani, M. H. Entezari, Photolysis and photocatalysis of methylene blue by ferrite bismuth nanoparticles under sunlight irradiation, Journal of Molecular Catalysis A: Chemical 377 (2013) 197–203.
[185] K. Ullah, Z. D. Meng, S. Ye, L. Zhu, W. C. Oh, Synthesis and characterization of novel PbS–graphene/TiO2 composite with enhanced photocatalytic activity, Journal of Industrial and Engineering Chemistry 20 (3) (2014) 1035–1042.

[186] A. Meng, B. Zhu, B. Zhong, L. Zhang, B. Cheng, Direct Z-scheme TiO2/CdS hierarchical photocatalyst for enhanced photocatalytic H2-production activity, Applied Surface Science 422 (2017) 518–527.
[187] R. K. Xu, S. C. Xiao, J. H. Yuan, A. Z. Zhao, Adsorption of methyl violet from aqueous solutions by the biochars derived from crop residues, Bioresource technology 102 (22) (2011) 10293–10298.
[188] S. G. Abuabara, L. G. Rego, V. S. Batista, Influence of thermal fluctuations on interfacial electron transfer in functionalized TiO2 semiconductors, Journal of the American Chemical Society 127 (51) (2005) 18234–18242.
[189] Pereira, L., Pereira, R., Oliveira, C. S., Apostol, L., Gavrilescu, M., Pons, M. N., ... & Madalena Alves, M. (2013). UV/TiO 2 photocatalytic degradation of xanthene dyes. *Photochemistry and Photobiology*, *89*(1), 33-39.
[190] Muhd Julkapli, N., Bagheri, S., & Bee Abd Hamid, S. (2014). Recent advances in heterogeneous photocatalytic decolorization of synthetic dyes. *The Scientific World Journal*, *2014*.
[191] L. R. Vargas, A. K. Poli, R. D. C. L. Dutra, C. B. D. Souza, M. R. Baldan, E. S. Gonçalves, Formation of composite polyaniline and graphene oxide by physical mixture method, Journal of Aerospace Technology and Management 9 (2017) 29–38.
[192] H. Tai, Y. Jiang, G. Xie, J. Yu, X. Chen, Z. Ying, Influence of polymerization temperature on NH3 response of PANI/TiO2 thin film gas sensor, Sensors and Actuators B: Chemical 129 (1) (2008) 319–326.
[193] S. Bingham, W. A. Daoud, Recent advances in making nano-sized TiO 2 visible-light active through rare-earth metal doping, Journal of Materials Chemistry 21 (7) (2011) 2041–2050.
[194] S. Jadoun, S. M. Ashraf, U. Riaz, Tuning the spectral, thermal and fluorescent properties of conjugated polymers via random copolymerization of hole transporting monomers, RSC advances 7 (52) (2017) 32757–32768.
[195] A. A. Ansari, M. A. M. Khan, M. N. Khan, S. A. Alrokayan, M. Alhoshan, M. S. Alsalhi, Optical and electrical properties of electrochemically deposited polyaniline/CeO2 hybrid nanocomposite film, Journal of Semiconductors 32 (4) (2011) 043001.
[196] Q. Hao, X. Xia, W. Lei, W. Wang, J. Qiu, Facile synthesis of sandwich-like polyaniline/boron-doped graphene nano hybrid for supercapacitors, Carbon 81 (2015) 552–563.
[197] R. S. Vikas, A. Sharma, A. K. Dhillon, S. Siddhanta, The Role of Metals in Nanocomposites for UV and Visible Light-Active Photocatalysis. *Green Photocatalytic Semiconductors*, Recent Advances and Applications (2021) 307.
[198] C. Yang, W. Dong, G. Cui, Y. Zhao, X. Shi, X. Xia, B. Tang, W. Wang, Highly-efficient photocatalytic degradation of methylene blue by PoPD-modified TiO2 nanocomposites due to photosensitization-synergetic effect of TiO2 with PoPD, Scientific Reports 7 (1) (2017) 1–12, doi:10.1038/s41598-017-04398-x.
[199] D. Yang, H. Liu, Z. Zheng, Y. Yuan, J. C. Zhao, E. R. Waclawik, H. Zhu, An efficient photocatalyst structure: TiO2 (B) nanofibers with a shell of anatase nanocrystals, Journal of the American Chemical Society 131 (49) (2009) 17885–17893.
[200] A. A. Abd El-Rady, Characterization and photocatalytic efficiency of palladium doped-TiO 2 nanoparticles, Advances in Nanoparticles 2 (04) (2013) 372.
[201] S. Sood, A. Umar, S. K. Mehta, S. K. Kansal, α-Bi2O3 nanorods: An efficient sunlight active photocatalyst for degradation of Rhodamine B and 2, 4, 6-trichlorophenol, Ceramics International 41 (3) (2015) 3355–3364.
[202] M. W. Shahzad, M. Burhan, K. C. Ng, Pushing desalination recovery to the maximum limit: Membrane and thermal processes integration, Desalination 416 (2017) 54–64.
[203] R. G. Saratale, G. D. Saratale, J. S. Chang, S. P. Govindwar, Bacterial decolorization and degradation of azo dyes: a review, Journal of the Taiwan institute of Chemical Engineers 42 (1) (2011) 138–157.
[204] X. H. Liu, Z. H. Xing, Q. Y. Chen, Y. H. Wang, Multi-functional photocatalytic fuel cell for simultaneous removal of organic pollutant and chromium (VI) accompanied with electricity production, Chemosphere 237 (2019) 124457.
[205] M. F. Hossain, S. Biswas, T. Takahashi, Y. Kubota, A. Fujishima, Effect of substrate temperature on the facing target sputter deposited Ti O 2 photoelectrode of dye-sensitized solar cells, Journal of Vacuum Science & Technology A: Vacuum, Surfaces, and Films 26 (4) (2008) 1012–1017.
[206] L. Jiang, X. Yuan, Y. Pan, J. Liang, G. Zeng, Z. Wu, H. Wang, Doping of graphitic carbon nitride for photocatalysis: a reveiw, Applied Catalysis B: Environmental 217 (2017) 388–406.
[207] K. Wang, Q. Li, B. Liu, B. Cheng, W. Ho, J. Yu, Sulfur-doped g-C3N4 with enhanced photocatalytic CO2-reduction performance, Applied Catalysis B: Environmental 176 (2015) 44–52.
[208] G. Buitrón, M. Quezada, G. Moreno, Aerobic degradation of the azo dye acid red 151 in a sequencing batch biofilter, Bioresource technology 92 (2) (2004) 143–149.
[209] K. Karthikeyan, K. Nanthakumar, K. Shanthi, P. Lakshmanaperumalsamy, Response surface methodology for optimization of culture conditions for dye decolorization by a fungus, Aspergillus niger HM11 isolated from dye affected soil, Iranian Journal of microbiology 2 (4) (2010) 213.
[210] Y. Lin, D. Li, J. Hu, G. Xiao, J. Wang, W. Li, X. Fu, Highly efficient photocatalytic degradation of organic pollutants by PANI-modified TiO2 composite, The Journal of Physical Chemistry C 116 (9) (2012) 5764–5772.
[211] Kumar, A., & Pandey, G. (2018). Synthesis, Characterization of Polypyrrole/Titania/GO by Co-Precipitation Method
[212] M. El Bouraie, El Din, Biodegradation of Reactive Black 5 by Aeromonas hydrophila strain isolated from dye-contaminated textile wastewater, Sustainable Environment Research 26 (5) (2016) 209–216.
[213] S. Ameen, M. S. Akhtar, H. S. Shin, Hydrazine chemical sensing by modified electrode based on in situ electrochemically synthesized polyaniline/graphene composite thin film, Sensors and Actuators B: Chemical 173 (2012) 177–183.
[214] DA Yaseen, M Scholz, Shallow pond systems planted with Lemna minor treating azo dyes, Ecol Eng 94 (2016) 295–305, doi:10.1016/j.ecoleng.2016.05.081.
[215] L.A. Bello, O. A. James, A. T. Oluwatosin, O. J. Akinropo, U. D. Oraeloka, A. E. Racheal, Treatment technologies for wastewater from cosmetic industry—A review, Int J Chem Biomol S 4 (4) (2018) 69–80.